Supporting Information

Towards two-photon absorbing dyes with unusually potentiated nonlinear fluorescence response

Carlos Benitez-Martin,[†,‡,#] Shiming Li,[†] Antonio Dominguez-Alfaro,[§,¶] Francisco Najera,[‡,#] Ezequiel Pérez-Inestrosa,[‡,#] Uwe Pischel,[§]* and Joakim Andréasson[†]*

† Department of Chemistry and Chemical Engineering, Physical Chemistry, Chalmers University of Technology, SE-412 96 Gothenburg, Sweden.
‡ Universidad de Málaga-IBIMA, Departamento de Química Orgánica, Campus Teatinos s/n, E-29071 Málaga, Spain.
# Centro Andaluz de Nanomedicina y Biotecnología (BIONAND), Parque Tecnológico de Andalucía, C/ Severo Ochoa 35, E-29590 Málaga, Spain.
§ CIQSO - Center for Research in Sustainable Chemistry and Department of Chemistry, University of Huelva, Campus de El Carmen s/n, E-21071 Huelva, Spain.

Table of Contents

General Methods and Materials for Synthesis

^{1}H, ^{13}C, DEPT and gHSQCAD NMR spectra were recorded on an Agilent 400 spectrometer at 25 °C. In the ^{1}H and ^{13}C NMR spectra chemical shifts (δ/ppm) are referenced to the residual solvent peak: $CDCl_3$, 7.26 ppm (^{1}H NMR), 77.2 ppm (^{13}C NMR); DMSO-d_6, 2.50 ppm (^{1}H NMR), 39.5 ppm (^{13}C NMR spectra). HRMS were obtained using an Agilent 1290 Infinity LC system tandem to an Agilent 6520 accurate mass Q-TOF LC/MS with an APCI source in positive mode. Thin-layer chromatography to monitor the reactions was performed on silica gel plates (Merck Kieselgel 60, F_{254}). The spots were made visible with UV light. Column chromatography was performed with silica gel (Merck silica 60). All chemicals and solvents [dimethylformamide (DMF), dichlormethane (DCM), methanol (MeOH), ethyl acetate (EtOAc), hexane] were purchased from commercial suppliers and used as received, unless stated otherwise. Tetrahydrofuran (THF) was distilled over Na/benzophenone and acetonitrile (MeCN) was distilled over CaH_2.

Synthesis of Compounds FL-DTE and FL-m

Synthesis of Compound FL-DTE

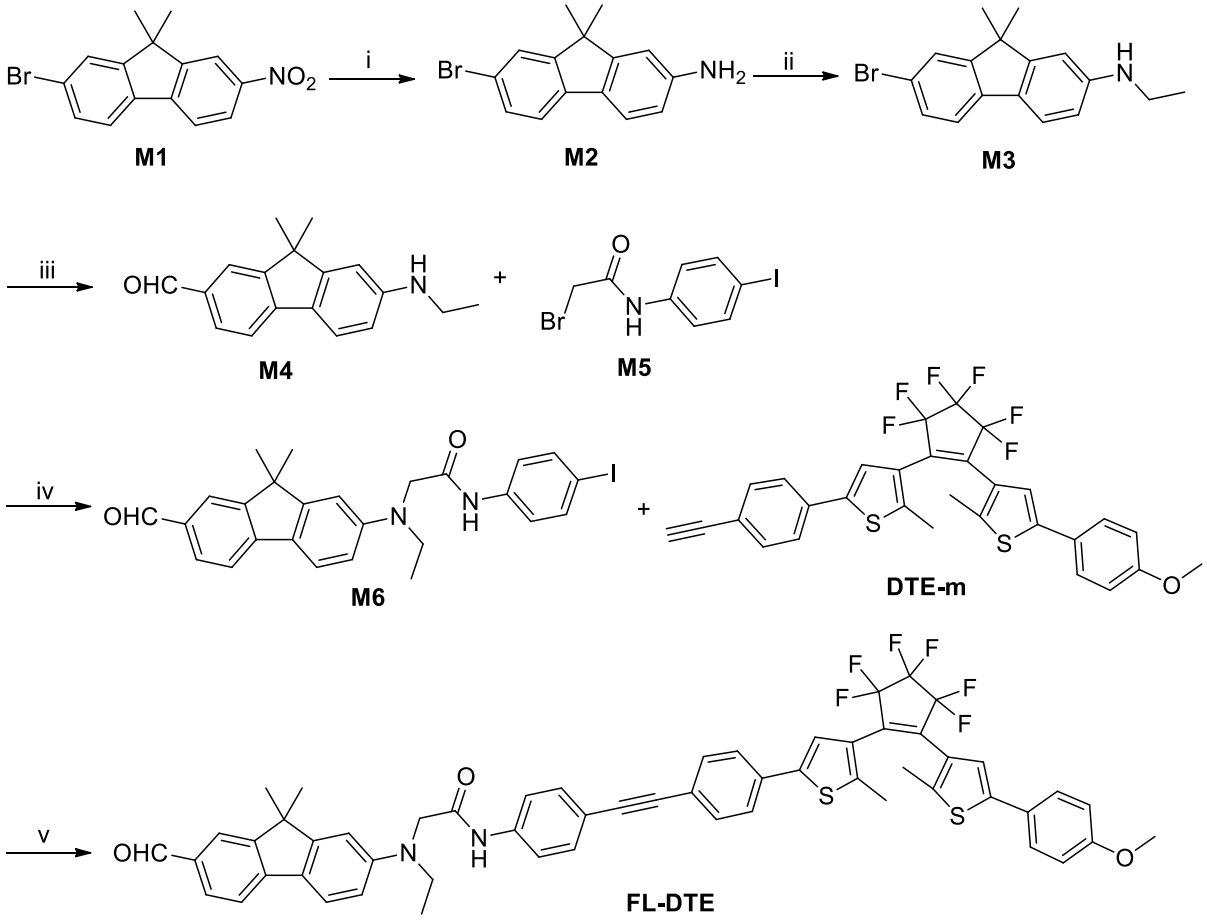

Scheme S1. Synthesis of compound **FL-DTE**. Reagents and conditions: (i) Fe powder, EtOH/H_2O, reflux, 2 h, N_2; (ii) EtI, K_2CO_3, DMF, 80 °C, 4 h; (iii) step 1. *tert*-BuLi, THF, -78 °C, Ar; step 2. DMF; (iv) Na_2HPO_4, NaI, MeCN, reflux, 18 h, Ar; (v) $Pd(PPh_3)_2Cl_2$, PPh_3, CuI, piperidine, THF, rt, 22 h, Ar.

7-Bromo-9,9-dimethyl-9*H*-fluoren-2-amine (M2)

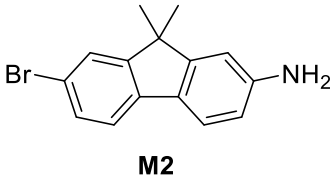

7-Bromo-9,9-dimethyl-9*H*-fluoren-2-amine (**M2**) was prepared by reduction of 2-bromo-9,9-dimethyl-7-nitro-9*H*-fluorene (**M1**) with iron powder in EtOH/H_2O according to a literature procedure.[1] The ^{1}H NMR data are consistent with the reported ones.

^{1}H NMR (400 MHz, DMSO-d_6) δ 7.62 (d, J = 1.6 Hz, 1H; Ar-H), 7.49 (d, J = 8.0 Hz, 1H; Ar-H), 7.45 (d, J = 8.4 Hz, 1H; Ar-H), 7.38 (dd, J = 8.0, 2.0 Hz, 1H; Ar-H), 6.65 (d, J = 2.0 Hz, 1H; Ar-H), 6.53 (dd, J = 8.4, 2.0 Hz, 1H; Ar-H), 5.31 (s, 2H; NH_2), 1.35 (s, 6H; C(CH_3)$_2$) ppm.
^{13}C NMR (101 MHz, DMSO-d_6) δ 154.7 (C_{quat}), 154.6 (C_{quat}), 149.3 (C_{quat}), 139.1 (C_{quat}), 129.5 (CH), 125.5 (CH), 125.46 (C_{quat}), 121.1 (CH), 119.8 (CH), 117.4 (C_{quat}), 112.9 (CH), 107.7 (CH), 46.3 (C_{quat}, C(CH$_3$)$_2$), 27.0 (2C; C(CH$_3$)$_2$) ppm.

7-Bromo-*N*-ethyl-9,9-dimethyl-9*H*-fluoren-2-amine (M3)

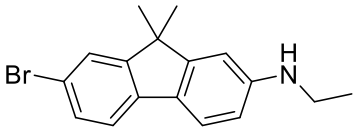

M3

In analogy to a literature procedure,[1] ethyl iodide (2.03 g, 13 mmol, 1 equiv.) was added to 7-bromo-9,9-dimethyl-9*H*-fluoren-2-amine (**M2)** (3.74 g, 13 mmol, 1 equiv.) and K_2CO_3 (1.80 g, 13 mmol) in DMF (30 mL). The reaction mixture was heated at 80 °C for 5 h. After cooling, the mixture was poured into H_2O and extracted with DCM. The organic phase was washed with H_2O, dried (over Na_2SO_4), and concentrated. The oily crude product was purified by flash chromatography (SiO_2, EtOAc/hexane, 1:4) to afford **M3** as a white solid (2.34 g, yield 57%).

^{1}H NMR (400 MHz, DMSO-d_6) δ 7.61 (d, J = 2.0 Hz, 1H; Ar-H), 7.50 (d, J = 8.0 Hz, 2H; Ar-H), 7.38 (dd, J = 8.0, 2.0 Hz, 1H; Ar-H), 6.65 (d, J = 2.0 Hz, 1H; Ar-H), 6.53 (dd, J = 8.0, 2.0 Hz, 1H; Ar-H), 5.77 (t, J = 5.6 Hz, 1H; NH), 3.09 (dq, J = 5.6, 7.2 Hz, 2H; CH_2CH$_3$), 1.37 (s, 6H; C(CH_3)$_2$), 1.18 (t, J = 7.2 Hz, 3H; CH$_2$CH_3) ppm.
^{13}C NMR (101 MHz, $CDCl_3$) δ 155.3 (C_{quat}), 154.9 (C_{quat}), 148.8 (C_{quat}), 139.1 (C_{quat}), 130.0 (CH), 127.9 (C_{quat}), 125.9 (CH), 121.2 (CH), 119.9 (CH), 118.8 (C_{quat}), 111.9 (CH), 106.8 (CH), 47.0 (C_{quat}, C(CH$_3$)$_2$), 38.8 (CH$_2$CH$_3$), 27.4 (2C; C(CH$_3$)$_2$), 15.0 (CH$_2$$CH_3$) ppm.

7-(Ethylamino)-9,9-dimethyl-9*H*-fluorene-2-carbaldehyde (M4)

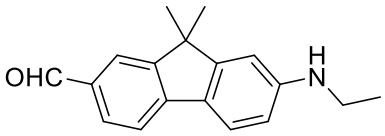

M4

A flask was charged with 7-bromo-*N*-ethyl-9,9-dimethyl-9*H*-fluoren-2-amine (**M3)** (0.90 g, 2.85 mmol), evacuated, and purged with Ar. Freshly distilled THF (40 mL) was added to the flask. To the light-yellow solution *tert*-BuLi (5.36 mL of 1.7 M solution in pentane, 9.12 mmol, 3.2 equiv.) was added dropwise at -78 °C. After the solution was stirred for 1 h, DMF (0.208 mg, 0.219 mL, 2.85 mmol, 1 equiv.) was added dropwise. The solution was stirred for additional 2 h at -78 °C and allowed to warm to room temperature for 1 h. H_2O was added to quench the reaction. The solution was extracted with EtOAc twice. The combined organic phase was dried (over Na_2SO_4) and concentrated under reduced pressure. The crude product was purified by flash chromatography (SiO_2, EtOAc/hexane, 1:4) to afford **M4** as a light yellow solid (0.43 g, yield 56%).

^{1}H NMR (400 MHz, $CDCl_3$) δ 9.99 (s, 1H, CHO), 7.89 (d, J = 0.8 Hz, 1H; Ar-H), 7.78 (dd, J = 8.0, 1.6 Hz, 1H; Ar-H), 7.65 (d, J = 8.0 Hz, 1H; Ar-H), 7.58 (d, J = 8.4 Hz, 1H; Ar-H), 6.65 (d, J = 2.4 Hz, 1H; Ar-H), 6.60 (dd, J = 8.4, 2.0 Hz, 1H; Ar-H), 3.94 (br s, 1H; NH), 3.25 (q, J = 7.2 Hz, 2H; CH_2CH$_3$), 1.48 (s, 6H; C(CH_3)$_2$), 1.30 (t, J = 7.2 Hz, 3H; CH$_2$CH_3) ppm.
^{13}C NMR (101 MHz, $CDCl_3$) δ 192.2 (CHO), 157.5 (C_{quat}), 153.4 (C_{quat}), 150.0 (C_{quat}), 146.9 (C_{quat}), 133.8 (C_{quat}), 131.3 (CH), 127.1 (C_{quat}), 122.59 (CH), 122.57 (CH), 118.5 (CH), 112.2 (CH), 106.4 (CH), 46.7 (C_{quat}, *C*(CH$_3$)), 38.6 (*C*H$_2$CH$_3$), 27.3 (2C; C(*C*H$_3$)$_2$), 14.9 (CH$_2$*C*H$_3$) ppm.

Bromo-*N*-4-iodophenylacetamide (M5)

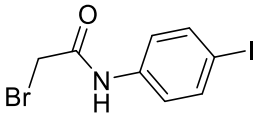

M5

Bromo-*N*-4-iodophenylacetamide (**M5**) was prepared according to a literature procedure.[2]

2-(Ethyl(7-formyl-9,9-dimethyl-9*H*-fluoren-2-yl)amino)-*N*-(4-iodophenyl)acetamide (M6)

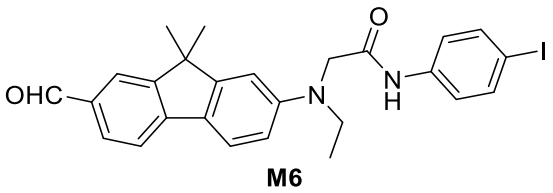

M6

In analogy to a literature procedure,[3] a flask was charged with 7-(ethylamino)-9,9-dimethyl-9*H*-fluorene-2-carbaldehyde (**M4**) (79 mg, 0.3 mmol, 1 equiv.), 2-bromo-*N*-4-iodophenylacetamide (**M5**) (102 mg, 0.3 mmol, 1 equiv.), Na_2HPO_4 (43 mg, 0.3 mmol, 1 equiv.), and NaI (18 mg, 0.12 mmol, 0.4 equiv.), evacuated, and purged with Ar. Freshly distilled MeCN (5 mL) was added to flask. The mixture was refluxed for 18 h under Ar. EtOAc (100 mL) was added to the brown reaction mixture solution, which then was washed with H_2O (3 × 50 mL) and brine (50 mL). The organic phase was dried (over Na_2SO_4) and concentrated under reduced pressure. The crude product was purified by flash chromatography (SiO_2, EtOAc/hexane, 1:4) to afford **M6** as a light yellow solid (118 mg, yield 75%).

^{1}H NMR (400 MHz, DMSO-d_6) δ 10.19 (s, 1H, NH), 9.94 (s, 1H, CHO), 7.93 (d, J = 0.8 Hz, 1H; Ar-H), 7.81 (dd, J = 8.0, 1.6 Hz, 1H; Ar-H), 7.77 (d, J = 7.6 Hz, 1H; Ar-H), 7.70 (d, J = 8.4 Hz, 1H; Ar-H),), 7.65 (m, 2H; Ar-H), 7.46 (m, 2H; Ar-H), 6.87 (d, J = 2.0 Hz, 1H; Ar-H), 6.65 (dd, J = 8.8, 2.4 Hz, 1H; Ar-H), 4.21 (s, 2H; CH_2CO), 3.57 (q, J = 6.8 Hz, 2H; CH_2CH$_3$), 1.41 (s, 6H; C(CH_3)$_2$), 1.19 (t, J = 6.8 Hz, 3H; CH_2CH_3) ppm.

^{13}C NMR (101 MHz, DMSO-d_6) δ 192.1 (CHO), 168.9 (C_{quat}), 156.7 (C_{quat}), 152.9 (C_{quat}), 149.4 (C_{quat}), 146.0 (C_{quat}), 138.6 (C_{quat}), 137.4 (2C; CH), 133.4 (CH), 130.5 (CH), 125.2 (C_{quat}), 122.54 (CH), 122.49 (CH), 121.6 (2C; CH), 118.5 (CH), 111.1 (CH), 105.6 (CH), 86.9 (C_{quat}), 53.9 (CH_2CO), 46.2 (C_{quat}, C(CH$_3$)$_2$), 45.9 (CH_2CH_3), 26.9 (2C; C(CH_3)$_2$), 12.1 (CH_2CH_3) ppm.

2-(Ethyl(7-formyl-9,9-dimethyl-9*H*-fluoren-2-yl)amino)-*N*-(4-((4-(4-(3,3,4,4,5,5-hexafluoro-2-(5-(4-methoxyphenyl)-2-methylthiophen-3-yl)cyclopent-1-en-1-yl)-5-methylthiophen-2-yl)phenyl)ethynyl)phenyl)acetamide (FL-DTE)

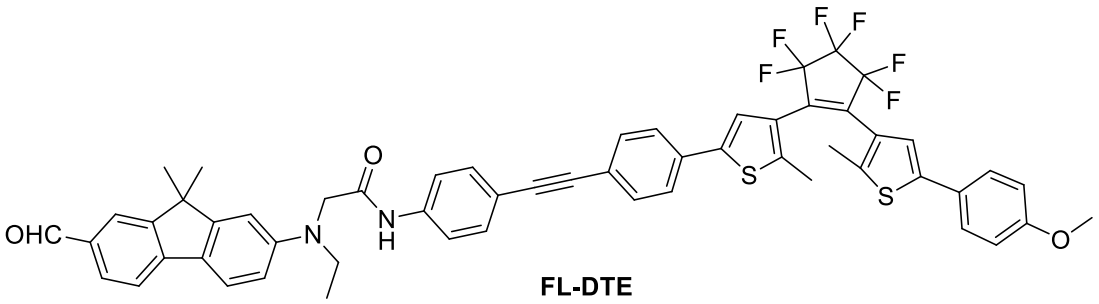

FL-DTE

In analogy to a literature procedure[4] a dry flask was charged with 2-(ethyl(7-formyl-9,9-dimethyl-9*H*-fluoren-2-yl)amino)-*N*-(4-iodophenyl)acetamide (**M6**) (79 mg, 0.15 mmol, 1 equiv.), CuI (3 mg, 0.15 mmol, 0.1 equiv.), $Pd(PPh_3)_2Cl_2$ (12 mg, 0.015 mmol, 0.1 equiv.), and PPh_3 (4 mg, 0.02 mmol, 0.1 equiv.). The flask was evacuated and purged with Ar. Freshly distilled THF (5 mL) bubbled with Ar and dry piperidine (0.4 mL) bubbled with Ar were added through a septum. After 15 min 1-[5'-(4"-methoxyphenyl)-2'-methylthien-3'-yl]-2-[2'-methyl-5'-(4"-ethynylphenyl)thien-3'-yl]-3,3,4,4,5,5-hexafluorocyclopentene (**DTE-m**)[5] (115 mg, 0.2 mmol, 1 equiv.) was added. The reaction mixture was stirred at room temperature for 22 h under Ar. Then the reaction solution was concentrated under reduced pressure. The residue was dissolved in DCM (100 mL), washed with H_2O (2 x 50 mL), dried (Na_2SO_4), and concentrated under reduced pressure. The crude product was purified by chromatography (SiO_2, EtOAc/DCM, 2:98) to afford **FL-DTE** (130 mg, yield 90%).

^{1}H NMR (400 MHz, $CDCl_3$) δ 10.01 (s, 1H, CHO), 8.31 (s, 1H; NH), 7.91 (dd, J = 1.6, 0.2 Hz, 1H; Ar-H), 7.82 (dd, J = 8.0, 1.6 Hz, 1H; Ar-H), 7.74-7.68 (m, 2H; Ar-H), 7.54-7.43 (m, 10H; Ar-H), 7.31 (br s, 1H; Thiophene-H), 7.15 (br s, 1H; Thiophene-H), 6.94-6.88 (m, 2H; Ar-H), 6.85 (d, J = 2.4 Hz, 1H; Ar-H), 6.81 (dd, J = 8.4, 2.4 Hz, 1H; Ar-H), 4.07 (s, 2H; CH_2CO), 3.84 (s, 3H; OCH_3), 3.64 (q, J = 7.2 Hz, 2H; CH_2CH$_3$), 1.97 (s, 3H; CH_3), 1.95 (s, 3H; CH_3), 1.49 (s, 6H; C(CH_3)$_2$), 1.33 (t, J = 7.2 Hz, 3H; CH$_2$CH_3) ppm.

^{13}C NMR (101 MHz, $CDCl_3$) δ 192.2 (CHO), 168.8 (CONH), 159.7 (C_{quat}), 157.57 (C_{quat}), 153.7 (C_{quat}), 148.9 (C_{quat}), 145.9 (C_{quat}), 142.4 (C_{quat}), 142.0 (C_{quat}), 141.6 (C_{quat}), 140.5 (C_{quat}), 137.3 (C_{quat}), 134.6 (C_{quat}), 133.2 (C_{quat}), 132.6 (2C; CH), 132.3 (2C; CH), 131.2 (CH), 129.2 (C_{quat}), 127.1 (2C; CH), 126.3 (C_{quat}), 126.3 (C_{quat}), 125.8 (C_{quat}), 125.5 (2C; CH), 123.1 (CH), 122.9 (CH), 122.84 (CH), 122.77 (C_{quat}), 121.4 (CH), 119.9 (2C; CH), 119.4 (C_{quat}), 119.2

(CH), 114.6 (2C; CH), 113.2 (CH), 107.8 (CH), 90.4 (C_{quat}), 89.2 (C_{quat}), 57.1 (CH_2CO), 55.6 (OCH_3), 47.1 (C_{quat}, $C(CH_3)_2$), 46.9 (CH_2CH_3), 27.3 (2C; $C(CH_3)_2$), 14.8 (CH_3), 14.7 (CH_3), 11.8 (CH_2CH_3) ppm. (Note: the carbons on the perfluropentene ring are not reported due to the very low intensities).

HRMS (Q-TOF, ESI^+, *m*/*z*): found $[M + H]^+$ = 971.2701; calcd for $[M + H]^+$ ($C_{56}H_{44}F_6N_2O_3S_2$) = 971.2770.

Synthesis of 2-(ethyl(7-formyl-9,9-dimethyl-9*H*-fluoren-2-yl)amino)-*N*-phenylacetamide (FL-m)

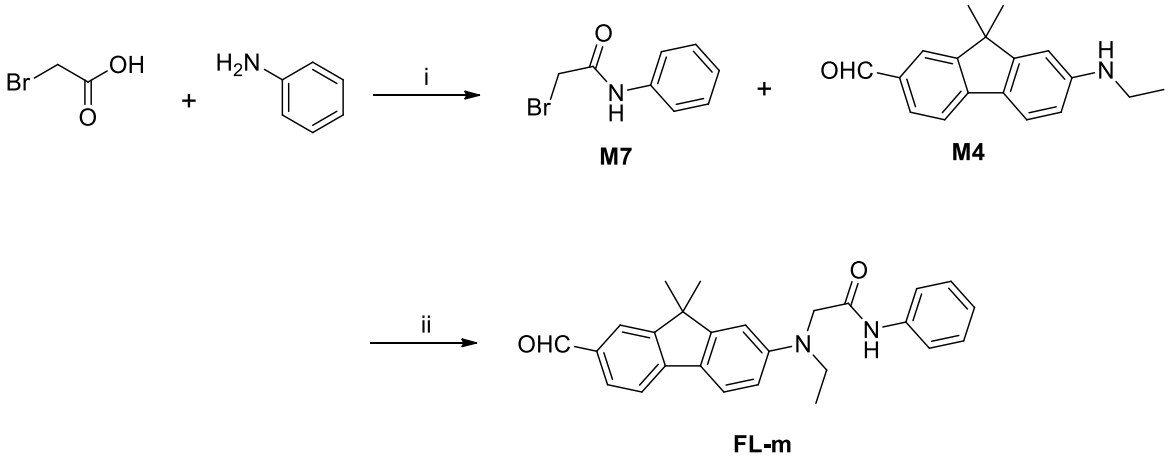

Scheme S2. Synthesis of compound **FL-m**. Reagents and conditions: (i) EDC-HCl, DCM, RT; (ii) Na_2HPO_4, NaI, MeCN, reflux, 18 h, Ar.

2-Bromo-*N*-phenylacetamide (M7)

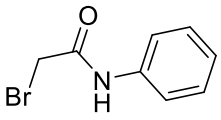

M7

Compound **M7** was prepared according to a literature procedure.[6] The ^1H NMR data are consistent with the reported ones.

2-(Ethyl(7-formyl-9,9-dimethyl-9*H*-fluoren-2-yl)amino)-*N*-phenylacetamide (FL-m)

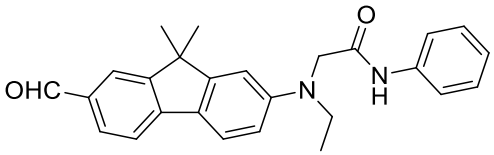

FL-m

In analogy to a literature procedure[3] a mixture of 7-(ethylamino)-9,9-dimethyl-9*H*-fluorene-2-carbaldehyde (**M4**) (86 mg, 0.33 mmol, 1 equiv.), 2-bromo-*N*-phenylacetamide (**M7**) (106 mg, 0.5 mmol, 1.5 equiv.), Na_2HPO_4 (71 mg, 0.5 mmol, 1.5 equiv.), and NaI (20 mg, 0.13 mmol, 0.4 equiv.) was added to a flask, evacuated, and purged with Ar. Freshly distilled MeCN (5 mL) was added to flask. The mixture was refluxed for 18 h under Ar. The organic phase was diluted with DCM, washed with H_2O, dried (over Na_2SO_4), and concentrated under reduced pressure. The crude brown oil was purified by flash chromatography (SiO_2, EtOAc/DCM, 1:4) to afford compound **FL-m** as a yellow solid (78 mg, yield 59%).

^{1}H NMR (400 MHz, $CDCl_3$) δ 10.00 (s, 1H, CHO), 8.23 (s, 1H; NH), 7.90 (d, J = 0.8 Hz, 1H; Ar-H), 7.81 (dd, J = 8.0, 1.6 Hz, 1H; Ar-H), 7.75-7.65 (m, 2H; Ar-H), 7.50-7.43 (m, 2H; Ar-H), 7.34-7.27 (m, 2H; Ar-H), 7.13-7.08 (m, 1H; Ar-H), 6.85 (d, J = 2.4 Hz, 1H; Ar-H), 6.81 (dd, J = 8.4, 2.4 Hz, 1H; Ar-H), 4.06 (s, 2H; CH_2CO), 3.63 (q, J = 7.2 Hz, 2H; CH_2CH$_3$), 1.48 (s, 6H; C(CH_3)$_2$), 1.32 (t, J = 7.2 Hz, 3H; CH$_2$CH_3) ppm.

^{13}C NMR (101 MHz, $CDCl_3$) δ 192.2 (CHO), 168.6 (C_{quat}), 157.5 (C_{quat}), 153.7 (C_{quat}), 149.0 (C_{quat}), 146.0 (C_{quat}), 137.2 (C_{quat}), 134.5 (C_{quat}), 131.2 (CH), 129.2 (2C, CH), 128.9 (C_{quat}), 125.0 (CH), 122.9 (CH), 122.8 (CH), 120.3 (2C; CH), 119.2 (CH), 113.1 (CH), 107.6 (CH), 57.0 (*C*H$_2$CO), 47.1 (C_{quat}, *C*(CH$_3$)$_2$), 46.8 (*C*H$_2$CH$_3$), 27.3 (2C; C(*C*H$_3$)$_2$), 11.9 (CH$_2$*C*H$_3$) ppm.

HRMS (Q-TOF, ESI$^+$, m/z): found $[M + H]^-$ = 399.2075; calcd for $[M + H]^-$ ($C_{26}H_{26}N_2O_2$) = 399.2067.

^{1}H, ^{13}C, DEPT and gHSQCAD NMR spectra and HRMS spectra

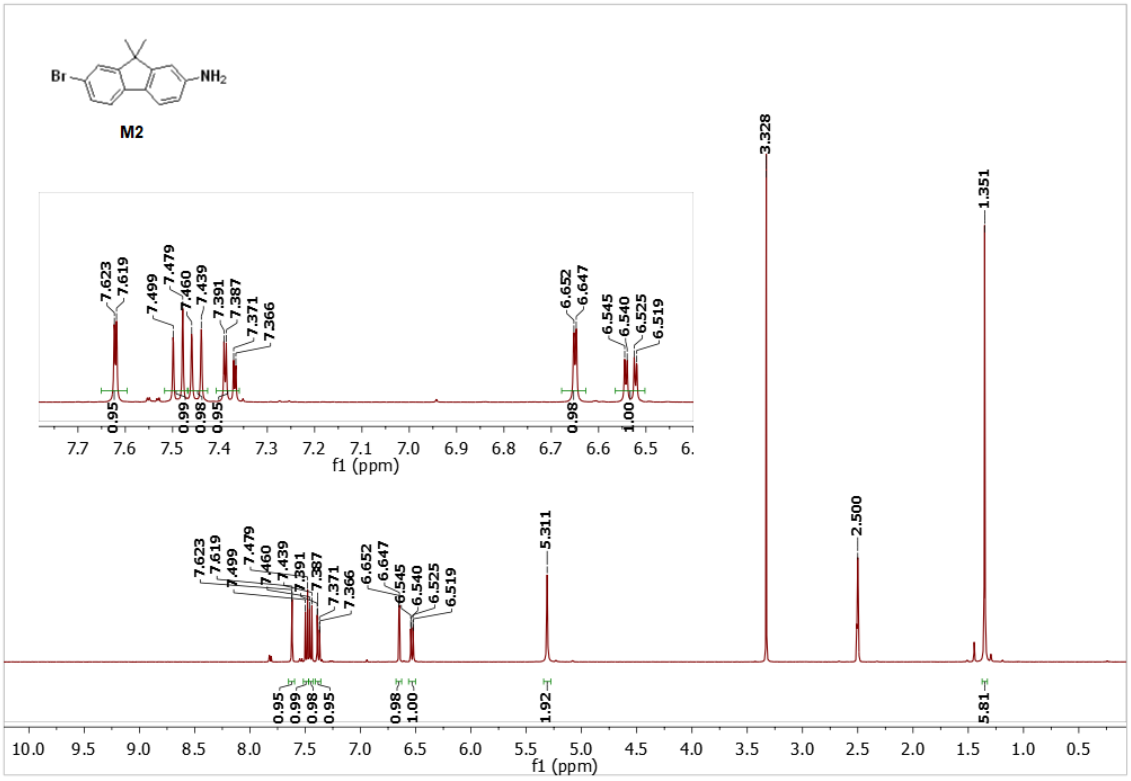

Figure S1. ^{1}H NMR spectrum (400 MHz, DMSO-d_6) of compound **M2**.

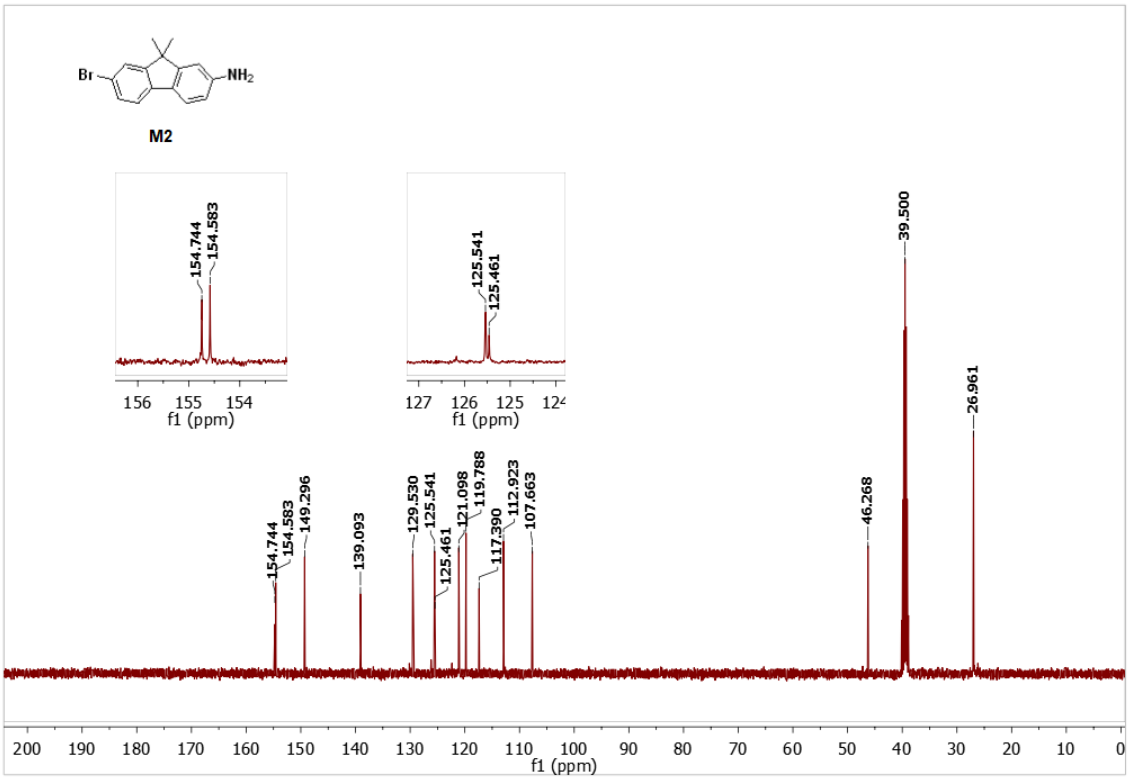

Figure S2. ^{13}C NMR spectrum (101 MHz, DMSO-d_6) of compound **M2**.

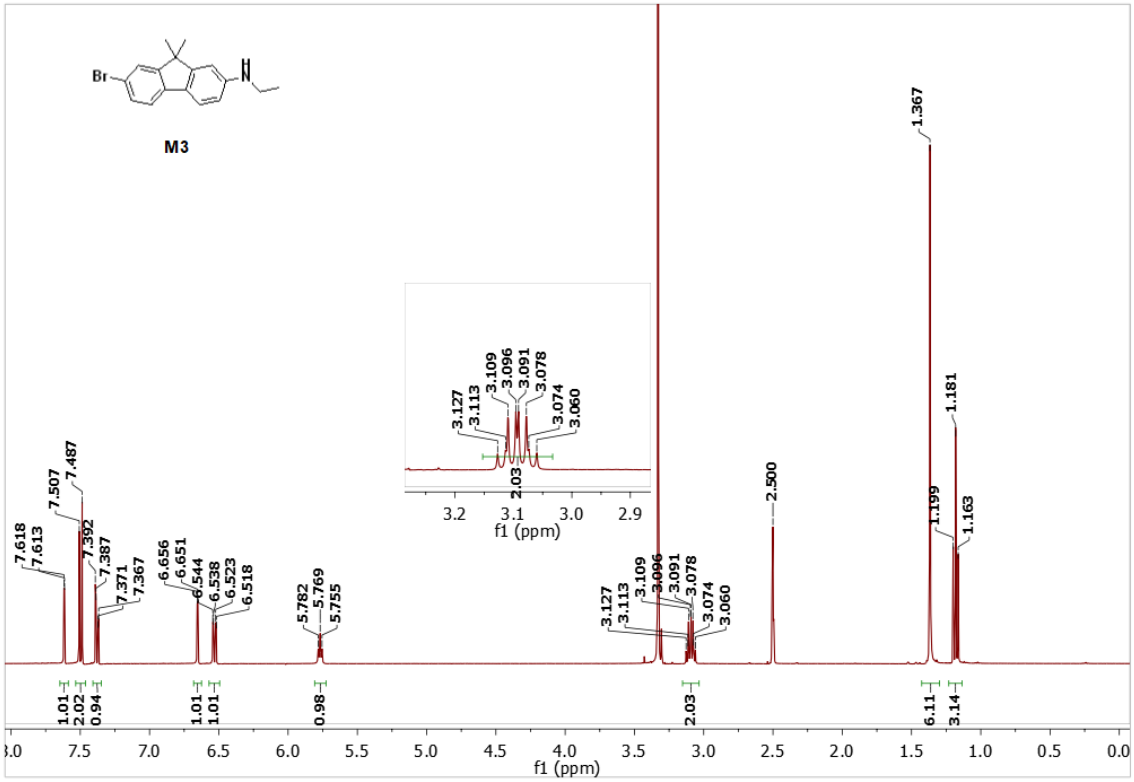

Figure S3. ^{1}H NMR spectrum (400 MHz, DMSO-d_6) of compound **M3**.

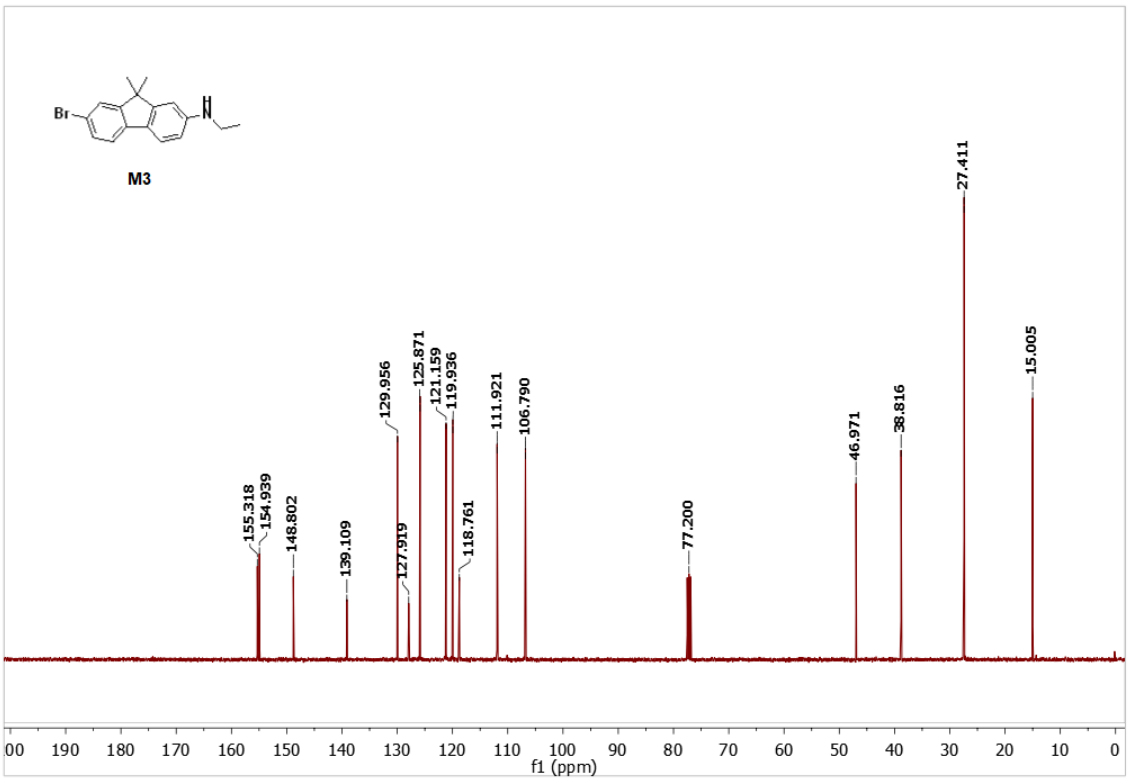

Figure S4. ^{13}C NMR spectrum (101 MHz, $CDCl_3$) of compound **M3**.

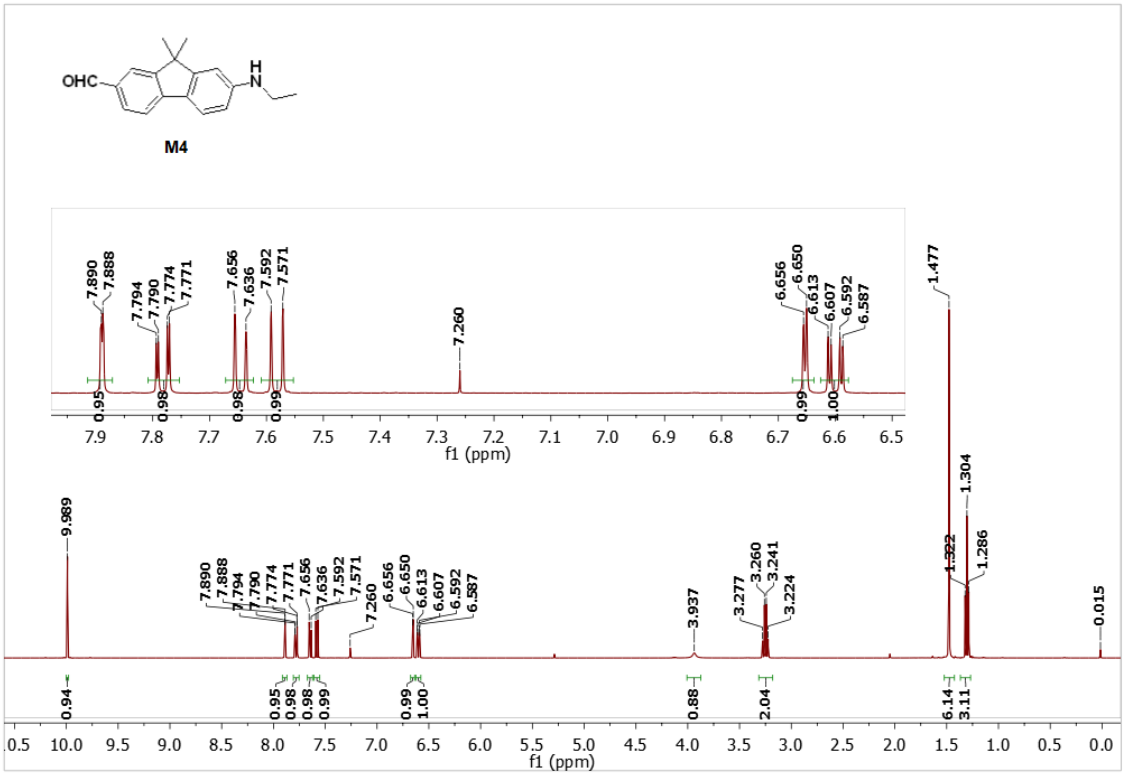

Figure S5. ^{1}H NMR spectrum (400 MHz, $CDCl_3$) of compound **M4**.

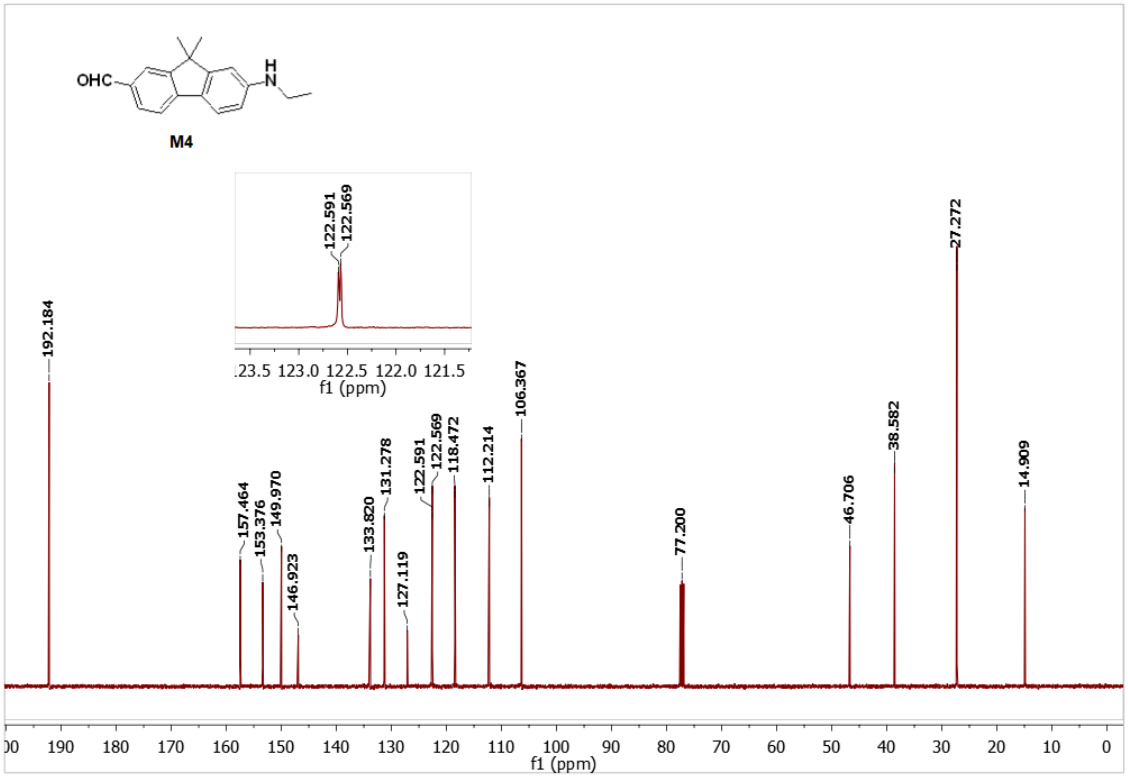

Figure S6. ^{13}C NMR spectrum (101 MHz, $CDCl_3$) of compound **M4**.

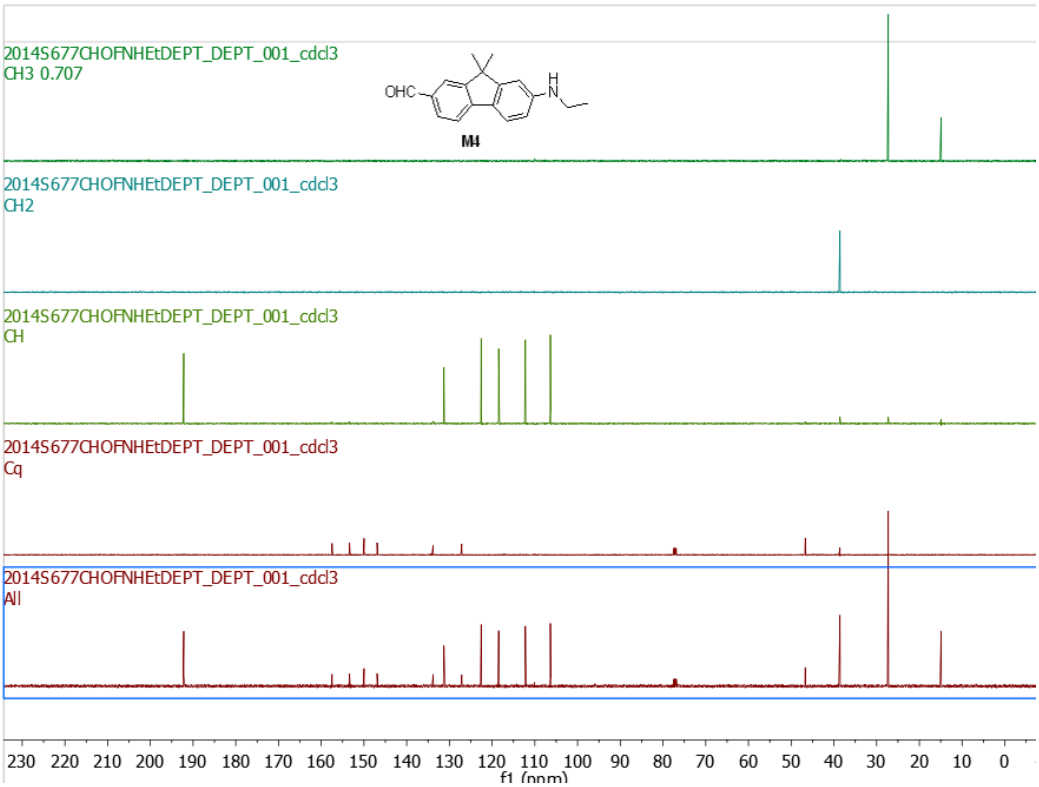

Figure S7. DEPT spectrum (101 MHz, $CDCl_3$) of compound **M4**.

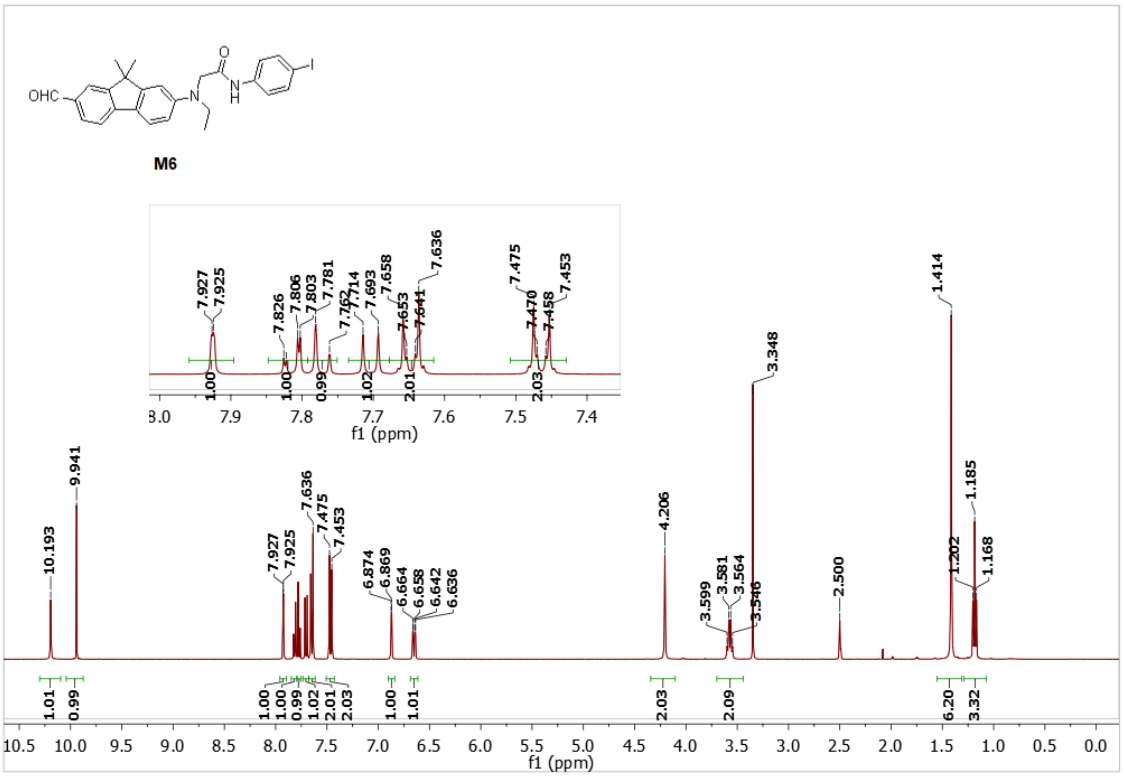

Figure S8. ^{1}H NMR spectrum (400 MHz, DMSO-d_6) of compound **M6**.

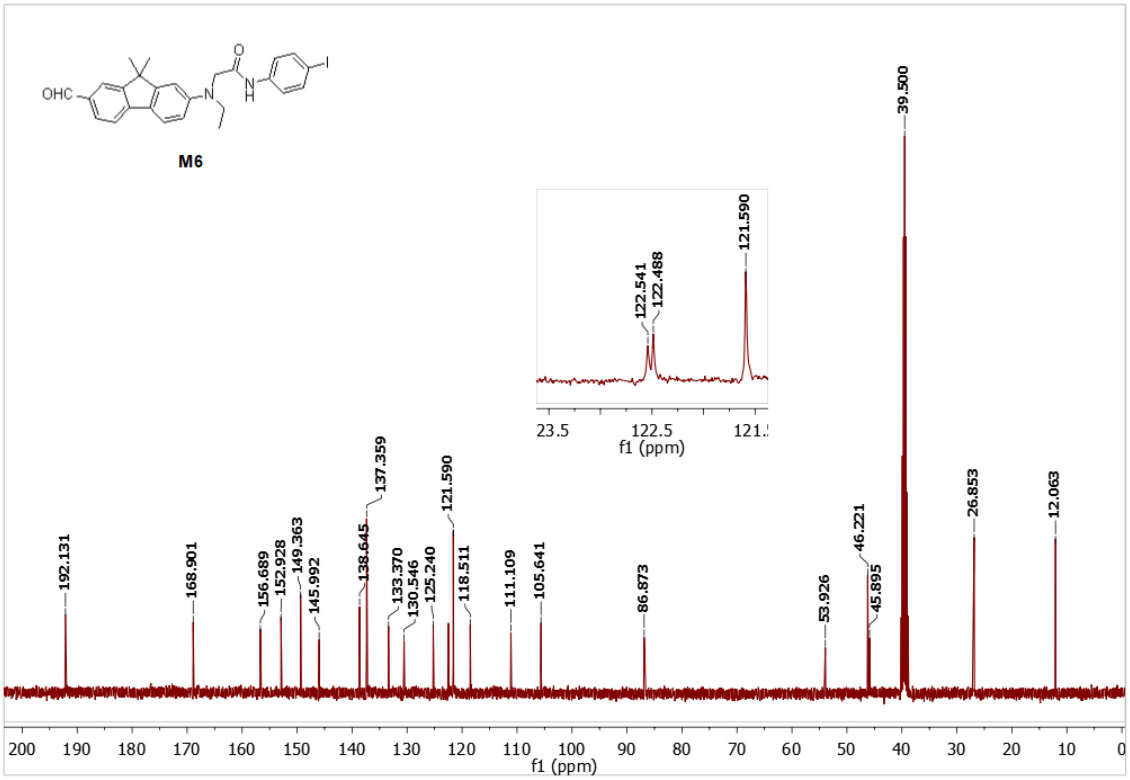

Figure S9. ^{13}C NMR spectrum (101 MHz, DMSO-d_6) of compound **M6**.

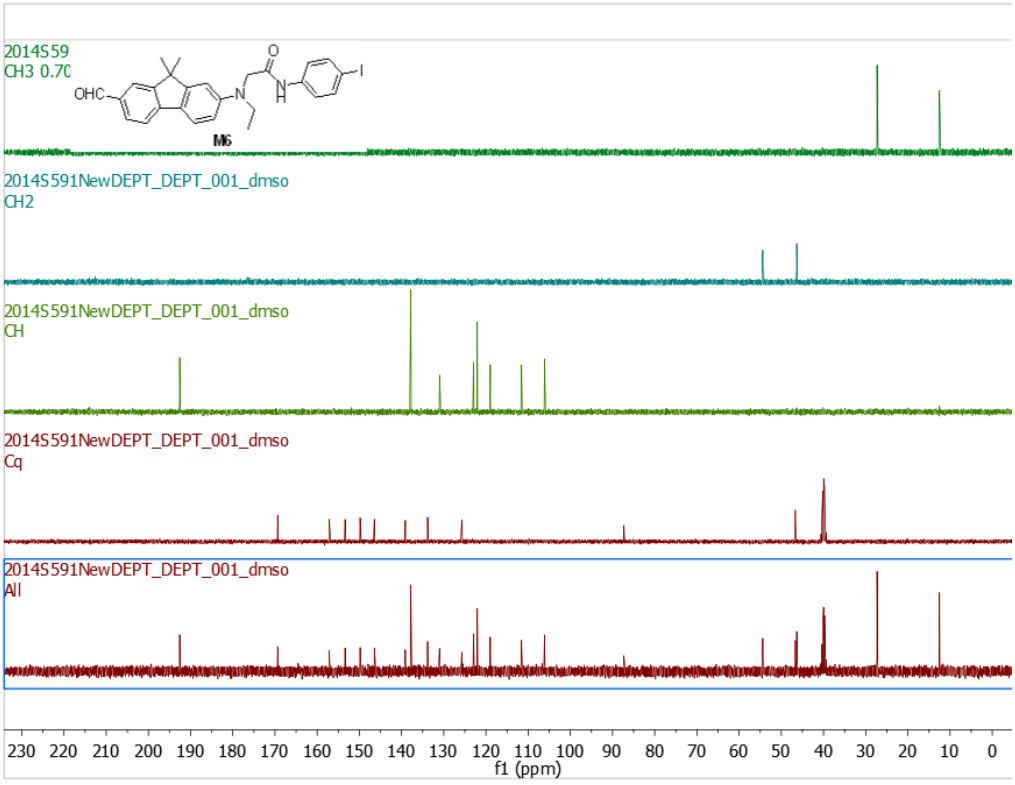

Figure S10. DEPT spectrum (101 MHz, $CDCl_3$) of compound **M6**.

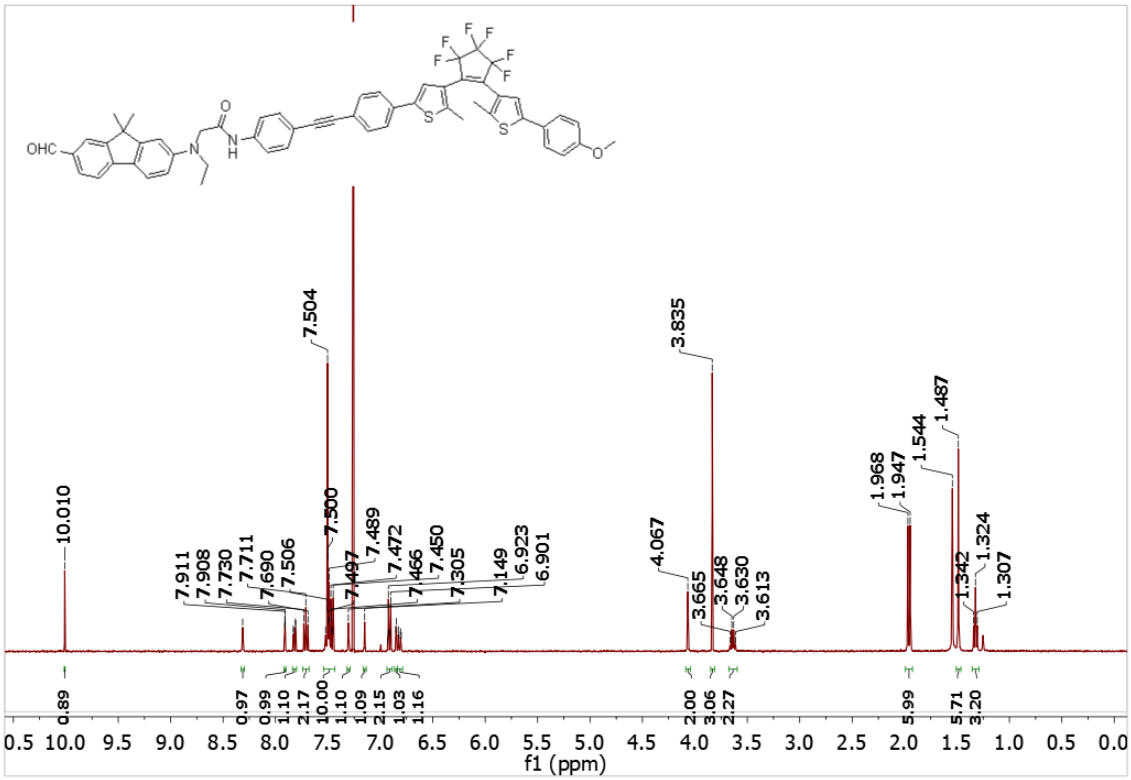

Figure S11. ^{1}H NMR spectrum (400 MHz, $CDCl_3$) of compound **FL-DTE** (δ 0 – 10).

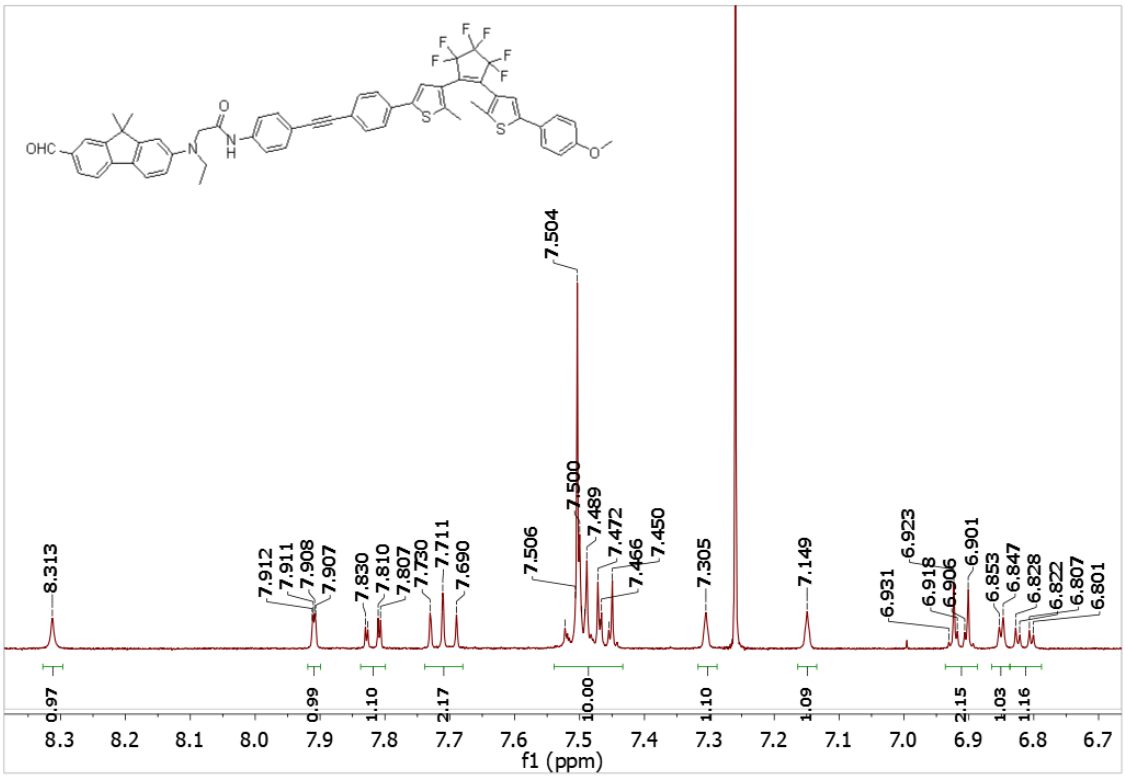

Figure S12. ^{1}H NMR spectrum (400 MHz, $CDCl_3$) of compound **FL-DTE** (δ 8.5 – 6.5).

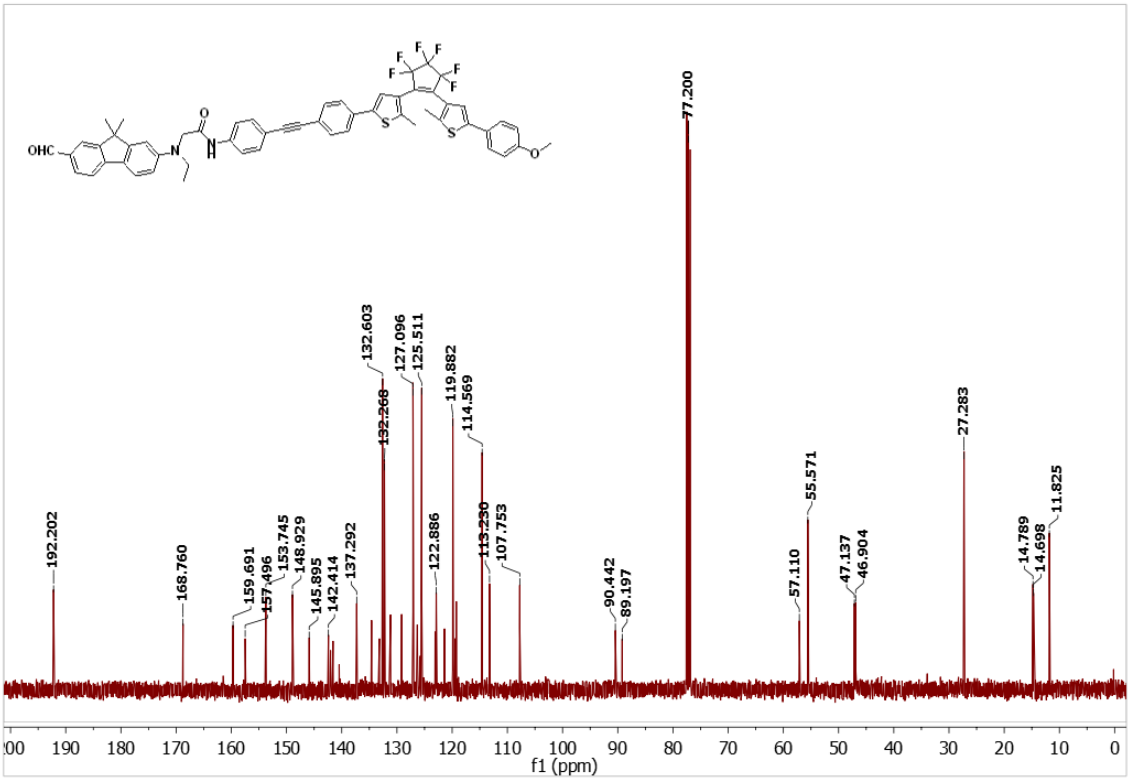

Figure S13. ^{13}C NMR spectrum (101 MHz, $CDCl_3$) of compound **FL-DTE** (δ 0 – 200).

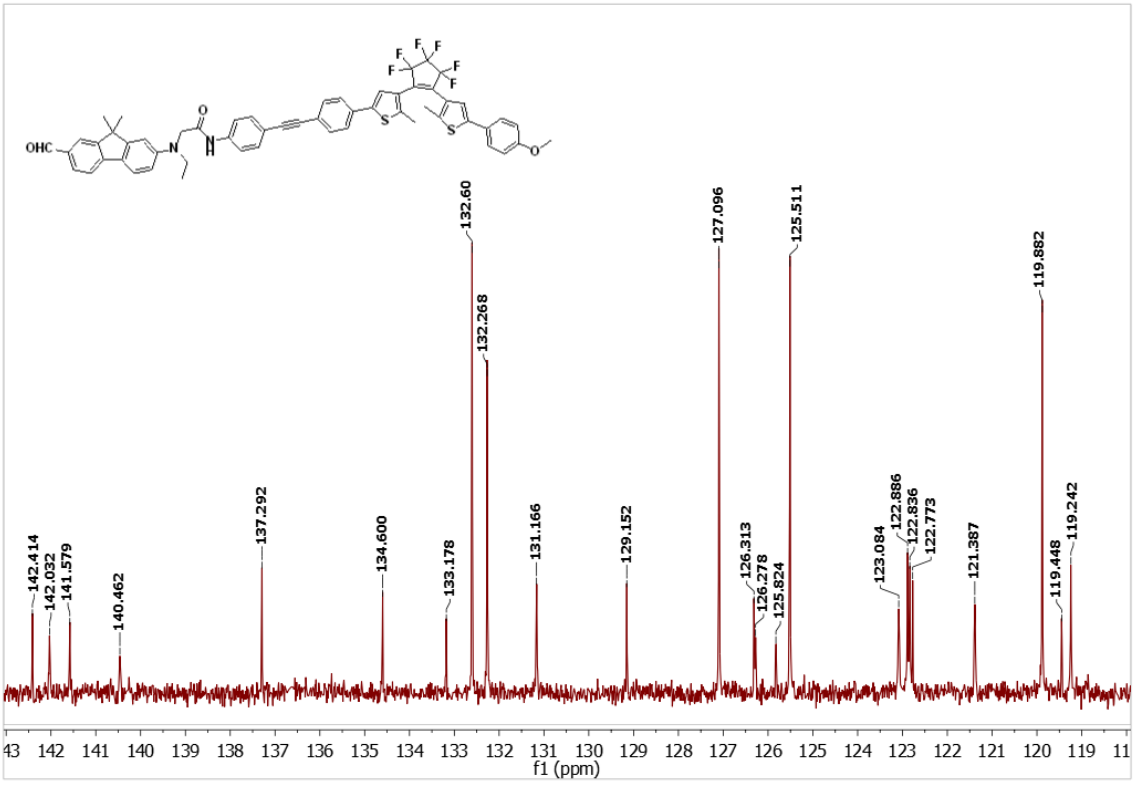

Figure S14. ^{13}C NMR spectrum (101 MHz, $CDCl_3$) of compound **FL-DTE** (δ 143 – 118).

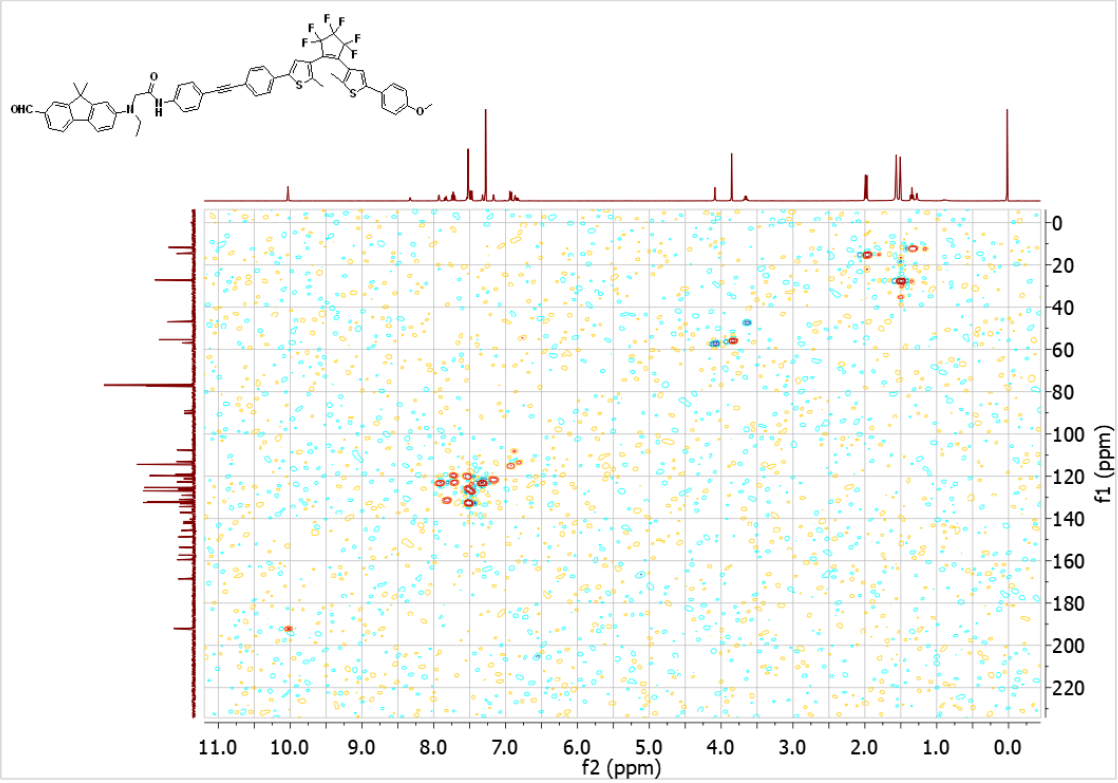

Figure S15. ^{1}H-^{13}C-gHSQCAD NMR spectrum (101 MHz, $CDCl_3$) of compound **FL-DTE**.

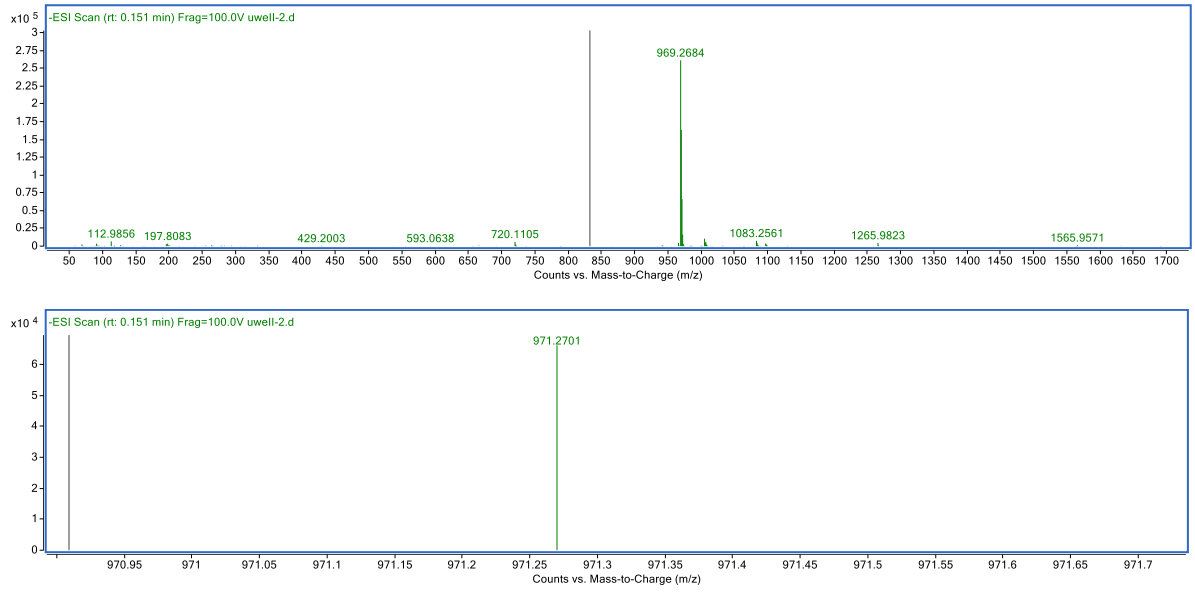

Figure S16. HRMS of compound **FL-DTE**.

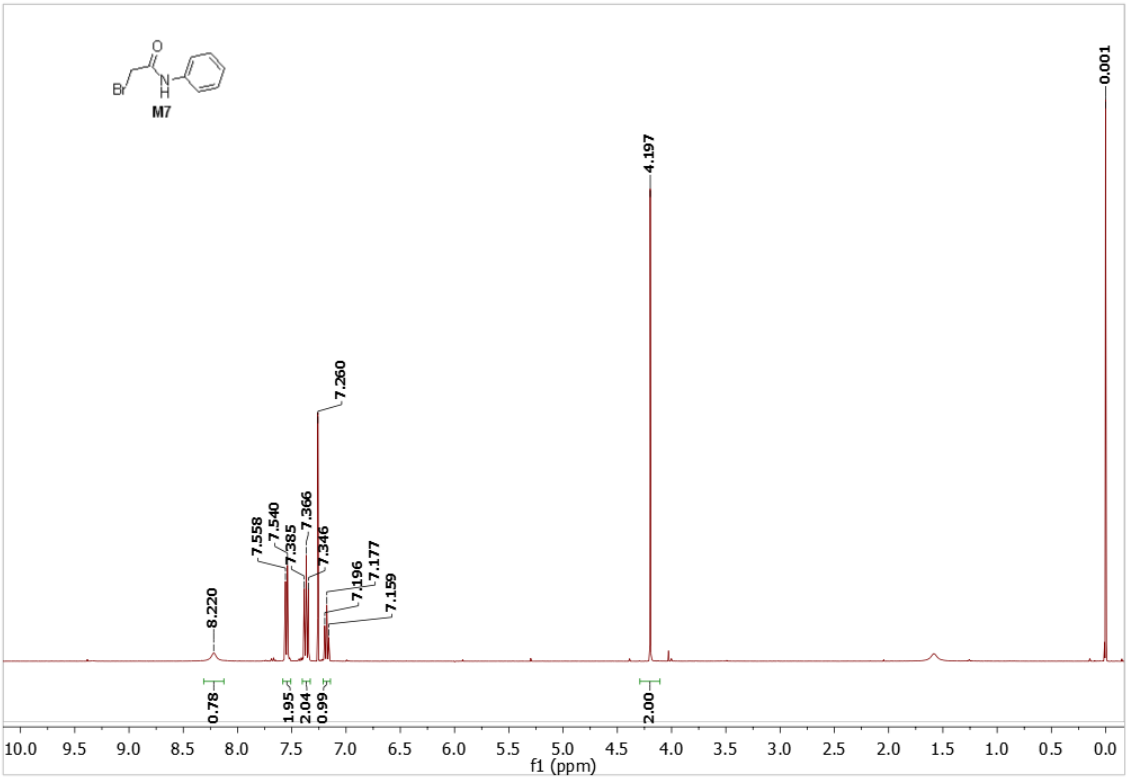

Figure S17. ^{1}H NMR spectrum (400 MHz, $CDCl_3$) of compound **M7**.

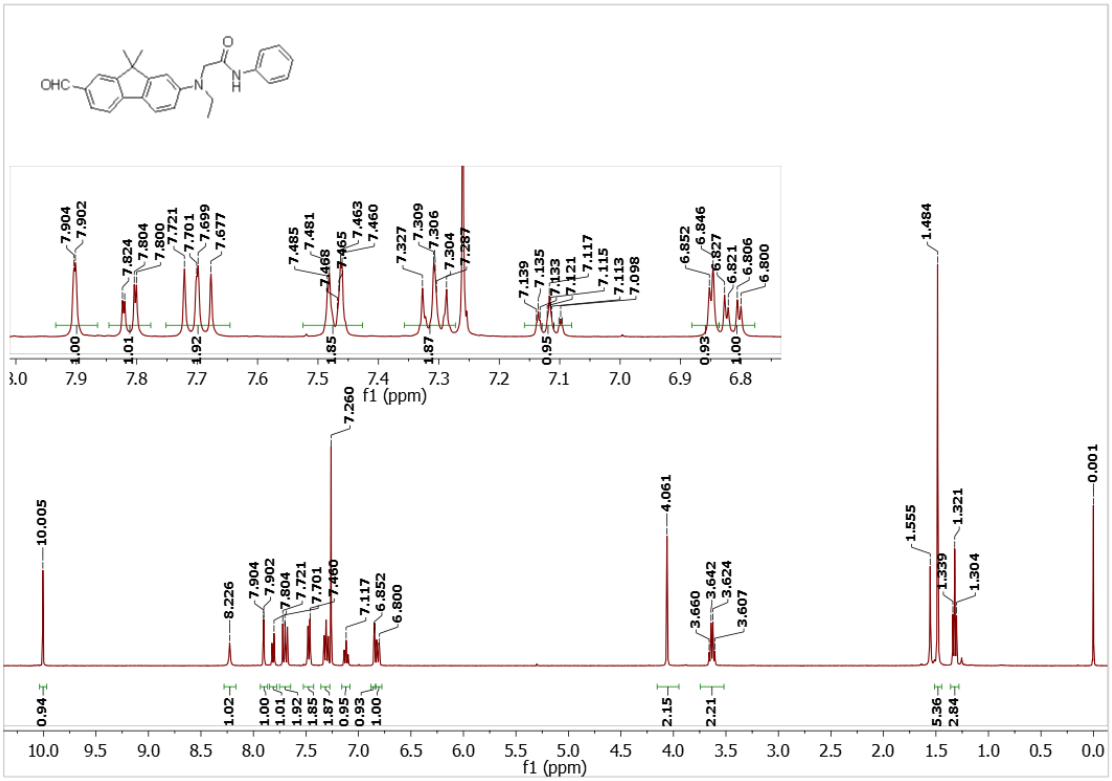

Figure S18. ^{1}H NMR spectrum (400 MHz, $CDCl_3$) of compound **FL-m**.

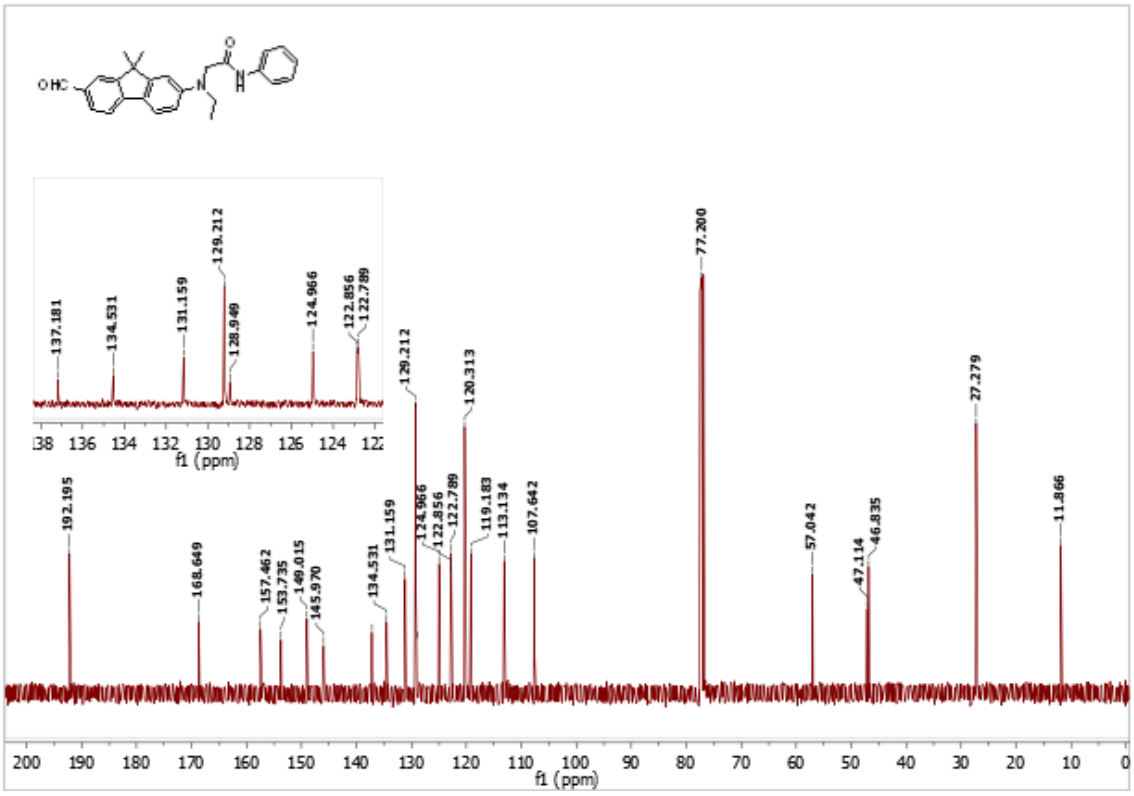

Figure S19. ^{13}C NMR spectrum (101 MHz, $CDCl_3$) of compound **FL-m**.

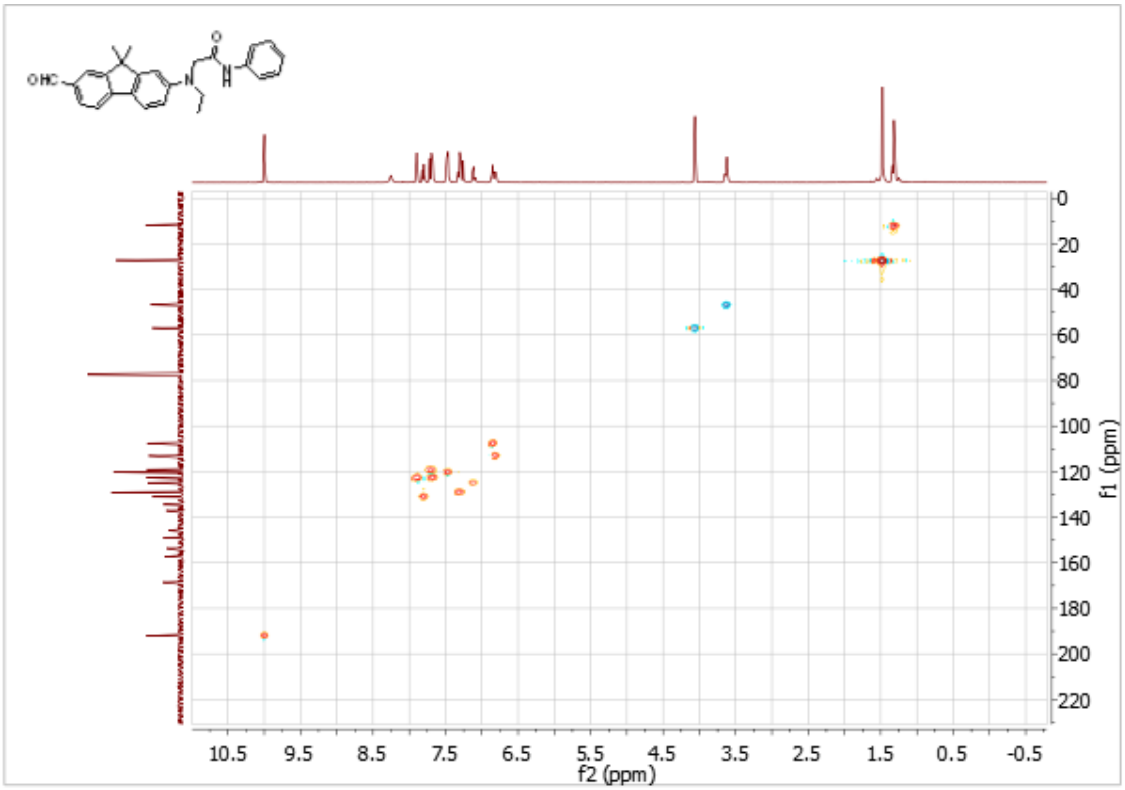

Figure S20. ^{1}H-^{13}C-gHSQCAD NMR spectrum (101 MHz, $CDCl_3$) of compound **FL-m**.

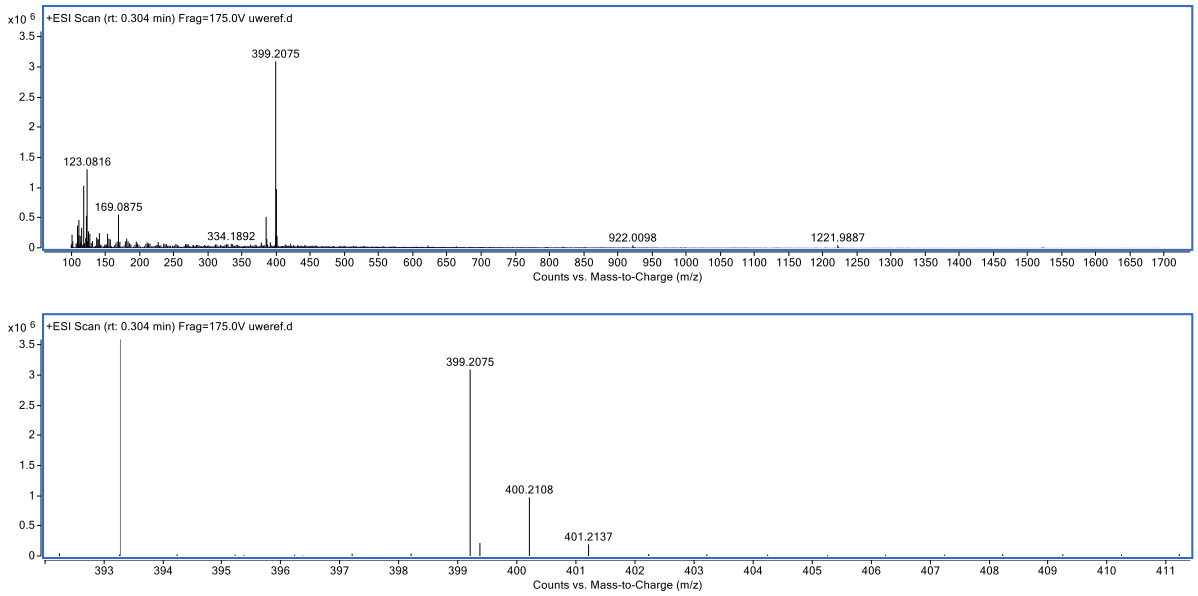

Figure S21. HRMS of compound **FL-m**.

One-Photon Spectroscopic Measurements

Spectroscopic grade methanol was used for all the photophysical measurements. The experiments were performed at room temperature with aerated and optically diluted methanol solutions, contained in a quartz cuvette of 1 cm pathlength.

The UV/vis absorption spectra were recorded using a Varian CaryBio 50 UV/vis spectrophotometer. Steady-state fluorescent measurements were recorded on a SPEX Fluorolog-3 spectrofluorometer (JY Horiba) or a Varian Cary Eclipse spectrofluorometer.

The fluorescence quantum yields (Φ_f) were determined according to literature procedure.[7] Coumarin 153 in ethanol (Φ_f = 0.38) was employed as the reference in all cases.

Fluorescence lifetimes were determined using a time-correlated single-photon-counting (TC-SPC) setup. The excitation light (λ_{exc} = 377 nm) was provided at a repetition rate of 20 MHz by a diode laser (LDH-P-C-375) powered by a PDL 800B pulsed diode driver (Picoquant, GmbH Germany). The emitted photons were collected at the magic angle (54.7°) at around the emission maxima by a thermoelectrically cooled microchannel plate photomultiplier tube (R3809U-50, Hamamatsu). The signal was digitalized using a multi-channel analyzer with 4096 channels (SPC-300, Edinburgh Analytical Instruments) and to ensure good statistics 10000 counts were recorded in the top channel. The measured fluorescence decays were fitted after deconvolution of the data with the instrument response function (IRF).

UV/vis and Fluorescence Spectra in One-Photon Conditions

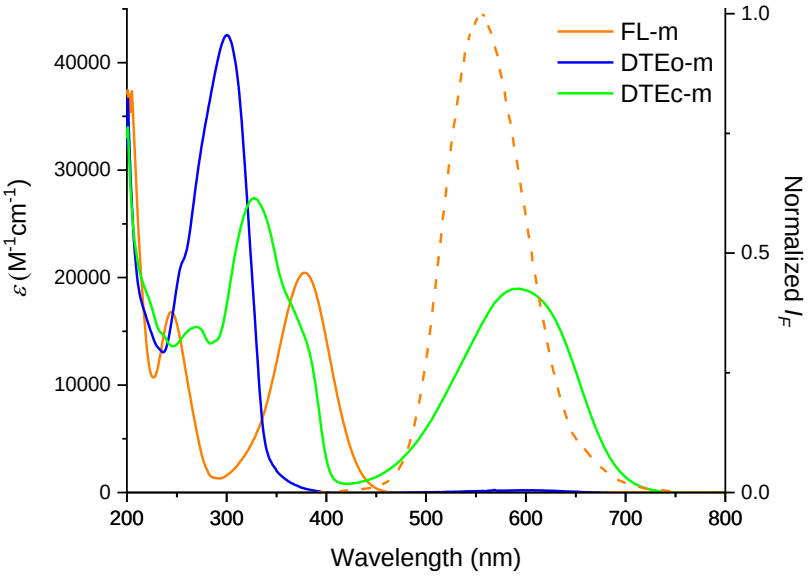

Figure S22. Absorption spectra (solid lines) of the model compounds in methanol (**FL-m**, orange line; **DTEo-m**, blue line; **DTEc-m**, green line). In addition the emission spectrum of **FL-m** is shown as dashed orange line.

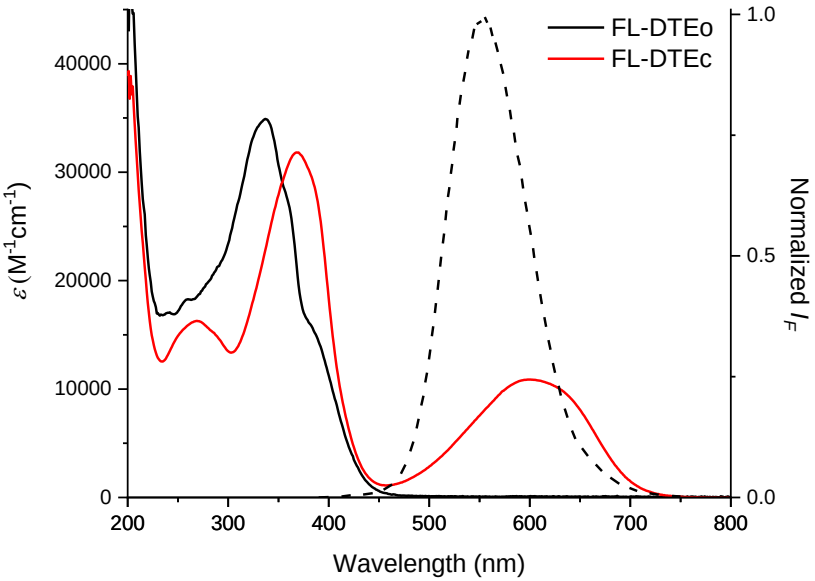

Figure S23. Absorption spectra (solid lines) of the dyad in both isomeric forms in methanol (**FL-DTEo**, black line; **FL-DTEc**, red line). The **FL-DTEo** emission spectrum is shown as dashed black line.

FRET and TD-DFT Calculations

Calculations were made with the Gaussian 16.A.03 package.[8] **FL-DTEc** geometrical parameters at the ground state (S_0) were optimized by means of density-functional theory (DFT), employing the Coulomb attenuated CAM-B3LYP[9] functional with first a 6-31+G(d) basis set and then fine-tuned with a 6-311+G(d,p) basis set. The solvent effects, methanol in this case, were accounted by including the Polarizable Continuum Model (PCM).[10] The absence of negative frequency in analytical Hessian calculations corroborated the nature of the minimum. The center-to-center distance between the two chromophores was determined as 22 Å

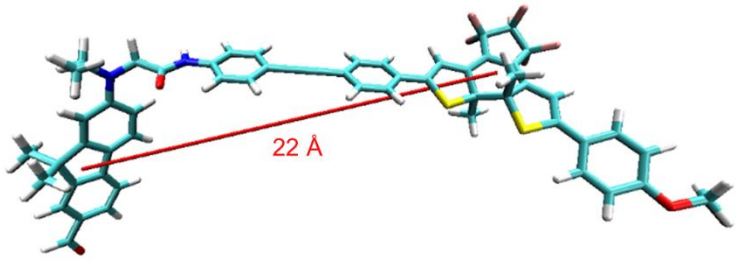

Figure S24. Optimized structure of the **FL-DTEc** dyad.

According to Förster theory,[11] the overlap integral (J) was calculated by using a|e - UV-Vis-IR Spectral Software,[12] returning a value of 1.54×10^{15} $nm^4\ M^{-1}\ cm^{-1}$. Assuming the orientation factor (κ^2) as 2/3, the critical Förster radius (R_0) was calculated as 48 Å. Hence, the FRET efficiency was estimated as practically quantitative ($\Phi_{FRET} = 0.99$).

The absorption energies were computed as vertical electronic excitations from the minima of the S_0 structures, using the linear-response (LR) approach with the time-dependent density functional response theory (TD-DFT).[13] This calculation was performed with the abovementioned functional and the 6-311+G(d,p) basis set for the ten first excited states. Natural Transition Orbitals (NTO),[14] which better describe the electronic movements in the electronic transitions, were represented. The transitions to the first (S_1) and the third (S_3) excited state were assigned to the absorptions of the DTEc and the FL moieties, respectively. The NTOs of these transitions are completely centered in the different chromophoric units that compose the dyad, thus, indicating the absence of electronic interactions among them.

Transition (NTO weight)	*NTO Hole*	*NTO Electron*
$S_0 \rightarrow S_1$ (92%)	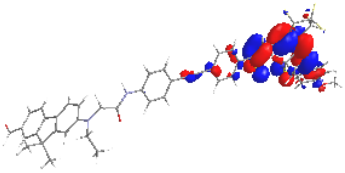	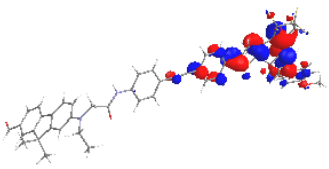
$S_0 \rightarrow S_3$ (90%)	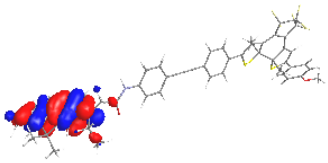	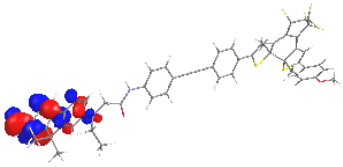

Table S1. NTO of **FL-DTEc**.

Transition (osc. strength)	$E_{theo,LR}$ *eV (nm)*	E_{exp} *eV (nm)*	*Contributions*
$S_0 \rightarrow S_1$ (0.855)	2.13 (581.81)	2.07 (600)	HOMO→LUMO (92%)
$S_0 \rightarrow S_3$ (1.016)	3.48 (356.79)	3.37 (368)	HOMO-1→LUMO+1 (87%)

Table S2. Calculated electronic and photophysical data for **FL-DTEc**.

From these transitions, dipole moment transitions (M) were used to correct κ^2. This was calculated as $\kappa^2 = (\cos\theta_{AD} - 3\cos\theta_A \cos\theta_D)^2 = 1.4844$ (see Figure S25).

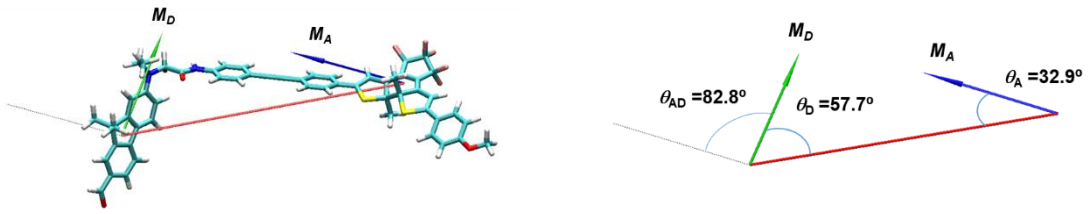

Figure S25. Dipole transitions moments abovementioned for **FL-DTEc** (left) and respective angles with the center-to-center vector.

Although this correction of the orientation factor yields a slightly higher and more accurate critical Förster radius of 53 Å, it does not imply any substantial change for the prediction of a quantitative FRET ($\Phi_{FRET} = 1$).

Atomic Coordinates for the Optimized Ground State of FL-DTEc

PCM(methanol)/CAM-B3LYP/6-31+G(d) level of theory

Energy (Hartree)	-3889.658667
Imaginary freq.	0

		Coordinates (Å)		
Atomic type		X	Y	Z
1	C	8.10914	-1.92825	0.84321
2	C	9.37701	-1.24084	0.65531
3	C	8.14163	0.56019	-0.47887
4	C	6.97427	0.22397	0.47493
5	C	6.92672	-1.29044	0.68921
6	C	8.35091	-3.34282	1.24881
7	C	9.88164	-3.54347	1.06115
8	C	10.48406	-2.1141	1.12932
9	C	9.44061	-0.0088	0.09795
10	C	10.55216	0.872	-0.08381
11	H	11.56962	0.57608	0.13943
12	C	10.21509	2.13134	-0.46873
13	C	7.96566	-0.02795	-1.89556
14	H	8.8609	0.17741	-2.48669
15	H	7.82451	-1.11099	-1.84848
16	H	7.1059	0.41422	-2.40079
17	C	7.10408	0.88836	1.86221
18	H	7.04626	1.97497	1.78525
19	H	6.29386	0.54129	2.50733
20	H	8.05552	0.62143	2.33001
21	S	8.47257	2.37115	-0.66178
22	C	11.12785	3.24997	-0.71124
23	C	12.48575	3.0239	-0.9642
24	C	10.67656	4.58055	-0.69552
25	C	13.37047	4.07246	-1.18284
26	H	12.86654	2.00917	-1.01164
27	C	11.54538	5.63382	-0.91022
28	H	9.63173	4.80011	-0.49751
29	C	12.90123	5.3884	-1.15467
30	H	14.41185	3.85232	-1.38159
31	H	11.19274	6.65973	-0.89051

32	O	13.67671	6.48008	-1.35645
33	C	15.06574	6.29572	-1.60701
34	H	15.47948	7.29545	-1.732
35	H	15.55373	5.79972	-0.76196
36	H	15.2254	5.71585	-2.52162
37	C	5.58856	-1.79972	0.71924
38	H	5.36253	-2.82274	0.99433
39	C	4.64582	-0.92231	0.29139
40	S	5.30217	0.64765	-0.19667
41	C	3.20293	-1.1665	0.191
42	C	2.60015	-2.1963	0.92944
43	C	2.39164	-0.38317	-0.64104
44	C	1.24099	-2.44038	0.83203
45	H	3.1958	-2.80227	1.60344
46	C	1.03024	-0.62304	-0.74293
47	H	2.82676	0.4178	-1.23063
48	C	0.43319	-1.65679	-0.00766
49	H	0.79167	-3.2373	1.41519
50	H	0.42007	-0.00872	-1.39653
51	C	-0.97056	-1.90265	-0.10552
52	C	-2.16144	-2.10742	-0.18914
53	F	10.41479	-4.38478	1.96564
54	F	10.11176	-4.05217	-0.17285
55	F	11.63072	-2.03437	0.40591
56	F	10.84047	-1.86515	2.43327
57	F	8.03864	-3.57639	2.56284
58	F	7.6533	-4.2675	0.53254
59	C	-3.56726	-2.34476	-0.28708
60	C	-4.17037	-3.39518	0.4218
61	C	-4.37752	-1.53328	-1.09109
62	C	-5.53244	-3.61802	0.32516
63	H	-3.56361	-4.03761	1.05137
64	C	-5.74547	-1.75038	-1.19265
65	H	-3.92879	-0.71606	-1.64656
66	C	-6.33502	-2.80058	-0.4812
67	H	-5.98175	-4.43559	0.88211
68	H	-6.35423	-1.11242	-1.8161
69	N	-7.71029	-3.09444	-0.52414
70	C	-8.70409	-2.47026	-1.22096

71	H	-7.99018	-3.8981	0.02569
72	O	-8.53931	-1.48119	-1.92018
73	C	-10.06945	-3.16012	-1.06825
74	H	-10.03379	-4.06931	-1.67505
75	H	-10.1966	-3.49465	-0.03089
76	N	-11.18948	-2.37097	-1.4995
77	C	-11.81366	-2.70413	-2.77706
78	H	-11.64891	-3.77135	-2.94804
79	H	-12.89677	-2.58275	-2.68195
80	C	-11.29031	-1.9112	-3.97296
81	H	-11.43905	-0.83582	-3.83795
82	H	-10.22074	-2.08628	-4.11644
83	H	-11.81928	-2.21829	-4.8817
84	C	-11.61407	-1.29015	-0.74738
85	C	-11.01001	-0.98635	0.49683
86	C	-12.6722	-0.46186	-1.18694
87	C	-11.45027	0.0707	1.28014
88	H	-10.1824	-1.57904	0.86534
89	C	-13.10225	0.58829	-0.39791
90	H	-13.14598	-0.63536	-2.14504
91	C	-12.50465	0.8653	0.83928
92	H	-10.95895	0.26589	2.22952
93	C	-14.21867	1.58179	-0.69707
94	C	-13.1668	2.02472	1.43097
95	C	-14.17292	2.45758	0.54831
96	C	-12.9449	2.68578	2.64251
97	C	-14.95705	3.54772	0.87261
98	C	-13.73487	3.77908	2.964
99	H	-12.16826	2.35236	3.32445
100	C	-14.74015	4.2157	2.08836
101	H	-15.73941	3.89797	0.20232
102	H	-13.58597	4.31169	3.89795
103	C	-13.91868	2.397	-1.96607
104	H	-12.95517	2.90977	-1.88787
105	H	-13.8892	1.74291	-2.84354
106	H	-14.69641	3.14953	-2.13236
107	C	-15.57759	0.8757	-0.83683
108	H	-15.57163	0.20148	-1.69944
109	H	-15.8117	0.28836	0.05632

110	H	-16.3781	1.60756	-0.98669
111	C	-15.58151	5.36936	2.41981
112	O	-15.49613	6.03546	3.4413
113	H	-16.34435	5.62801	1.66127

Isomerization Quantum Yield Determination

The isomerization quantum yields were determined according to standard procedures by using furylfulgide (Aberchrome 540^{TM}) as actinometer.[15] The ring-opening reactions were triggered using 523 nm from a LED (LZ4-00G108-0000). The closing reactions were carried out with a 302 nm handheld lamp (UVP 34004401). The absorbance changes in the dyad were monitored at 592 nm and compared to those of the reference compound at 494 nm under identical irradiation power/geometries. The molar absorption coefficients of either the dyad and the reference compound, at 302 nm for the open isomers and at 523 nm for the closed isomers, were used to correct the isomerization quantum yields of the closing and the opening reactions, respectively.

Two-Photon Fluorescence Microscopy

The fluorescence properties of the compounds were analyzed using a ZEISS LSM710 NLO MP/Confocal Microscope at the Centre of Cellular Imaging at Gothenburg University. This microscope is equipped with an InSight DS+ laser (Spectra-Physics) tunable between 680 nm and 1300 nm. The provided pulse width was 100 ps. Imaging was performed using a Plan-Apochromat 10x objective (NA 0.45) focused at the air/liquid boundary, allowing the simultaneous detection of sample and background fluorescence. Emission spectral data for compound and background regions of interest (ROIs) were registered using ImageJ software.

All compounds were dissolved in spectroscopic grade methanol and diluted to a concentration of 10 μM. Emission spectra were measured in a laser power regime where the fluorescence was proportional to the square of the laser excitation power and using a dynamic 10 nm wide emission detection window moving in 25 steps between 445 and 700 nm.

The two-photon absorption cross-sections (σ_{2PA}) were determined between 700 and 1000 nm by the two-photon-induced-fluorescence method.[16] Rhodamine B (5 μM in methanol) was used as a reference under experimentally identical conditions, assuming that the fluorescence quantum yield is the same regardless of whether two-photon or one-photon excitation is used.

Additional Two-Photon Absorption Data of Compounds FL-DTEo and FL-m

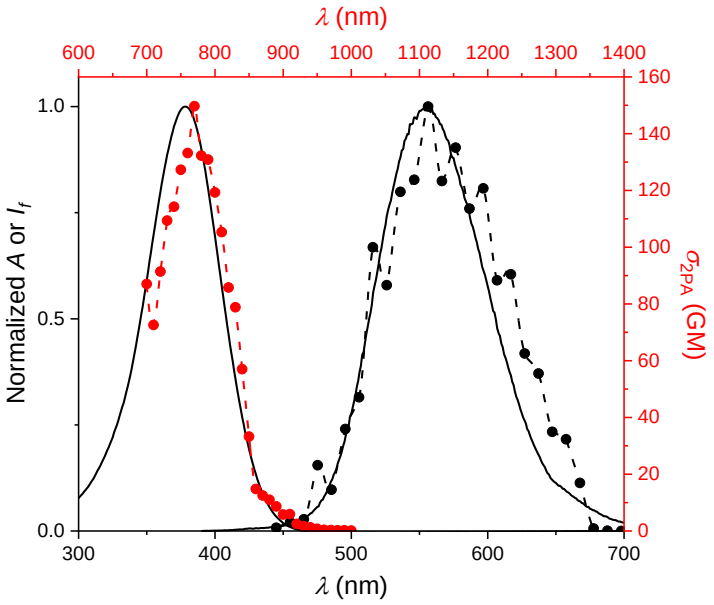

Figure S26. One-photon absorption (left) and fluorescence (right) spectra of **FL-m** (black solid lines); 10 μM in methanol. The energy-scaled two-photon absorption spectrum (red dashed line and red points) nicely coincides with the one under single-photon conditions. The two-photon-excited fluorescence spectrum (black dashed line and black points) coincides with the conventional fluorescence spectrum (black solid line).

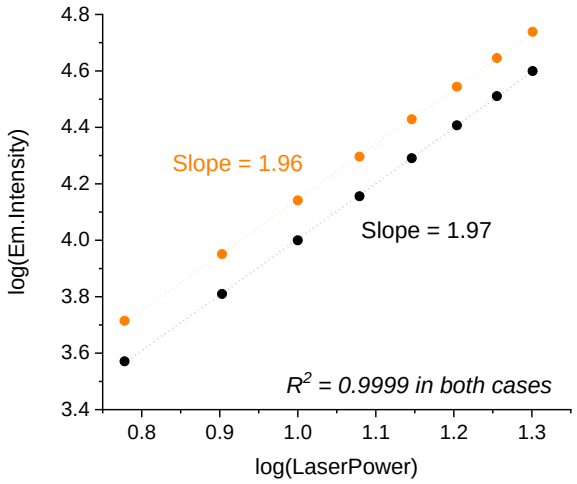

Figure S27. Double-logarithmic plot of the emission maximum intensity *versus* laser power for **FL-m** (orange points) and **FL-DTEo** (black points). The dashed lines represent the linear regression fittings. In both cases the slopes are close to 2, which indicate the two-photon absorption regime.

Two-Photon-Mediated Isomerization Studies

A **FL-DTEo** solution (10 μM in methanol) was irradiated with 302 nm light until the photostationary state was reached, being this process followed by UV/vis absorption. Approximately less than 1 μL of this solution was introduced inside 5 μL microcapillary tubes (Hirschmann). Theses tubes were employed in order to avoid as much as possible any diffusion phenomena. The capillaries were then sealed to avoid evaporation of the solvent. The isomerization process was followed by recording 500 images during 120 seconds, *i.e.*, 1 image each 240 msec. Excitation at 820 nm was carried out at half intensity and full intensity of the laser power at this wavelength. The images were processed as described above for the emission spectra, resulting in the curves displayed in the main text.

Modeling of the FI/HI Quotient

The generic expressions for the fluorescence intensity kinetics expected for HI (half laser intensity) and FI (full laser intensity; see Figure 3 in main text), assuming a quartic dependence are:

HI: $y = 1 - e^{-kt}$

FI: $y = 4\times(1-e^{-4kt})$

The quotient FI/HI was plotted (with *k* arbitrarily set to 1) under the assumption that X % of the open fluorescent isomer was present already at time = 0 (at the PSD after 302 nm exposure). With X = 6 %, the curve in Figure S28 resulted, with a maximum quotient of 10.1, being in coincidence with the experimental observations (see main text).

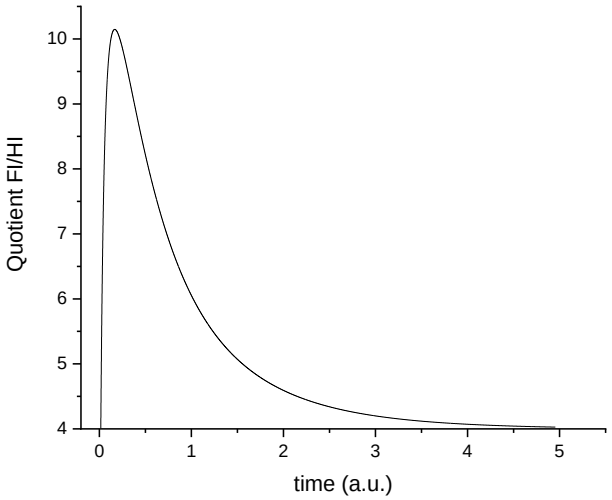

Figure S28. Modeling of the FI/HI quotient, assuming a presence of 6% open isomer in the initial state (time = 0).

The ratio of the fast kinetic components, ascribed to FRET-induced isomerization, is 4.2 (Figure S29). For a quartic dependence the ratio is expected to be 4.

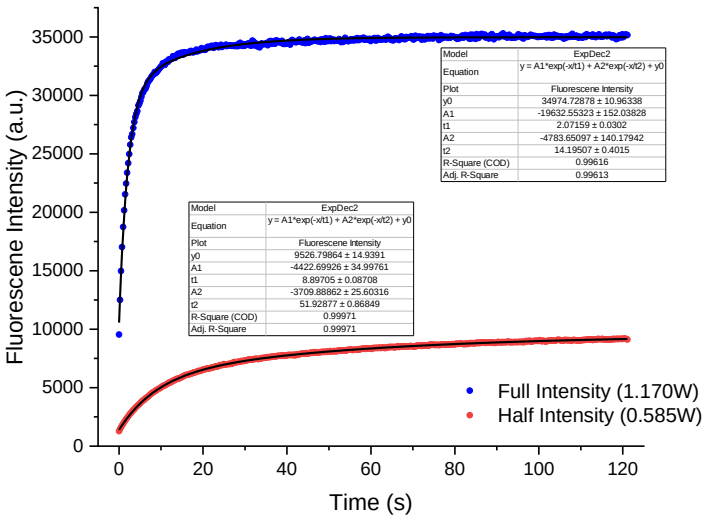

Figure S29. Biexponential fitting of the FI (blue) and HI (red) kinetic traces of fluorescence build-up on ring-opening isomerization of **FL-DTEc** under two-photon excitation.

Evaluation of the Possibility of Photoinduced Electron Transfer in the FL-DTE Dyad

In order to evaluate the possibility of the occurrence of photoinduced electron transfer (PET) from excited singlet state fluorene to the isomeric forms of the DTE moiety in the dyad we employed the Rehm-Weller equation ($\Delta G = E_{ox} - E_{red} - E^* + C$). Redox potentials are commonly available for acetonitrile or DMF, which are comparable in their polarity with methanol, being the solvent of our study. The reduction potentials (*vs.* SCE reference) for a DTE model are available from the literature; E_{red} (DTEo) ≈ −2.3 V and E_{red} (DTEc) ≈ −1.8 V.[17] The excitation energy of the fluorene moiety was estimated as E^* ≈ 2.8 eV, according to a published approach for ICT fluorophores.[18] The oxidation potential of the push-pull fluorene moiety is unfortunately not available. However, using the redox potential of an electronically related push-pull aromatic system (such as 4-methylcarboxy-*N*,*N*-dimethylaniline or 4-trifluoromethyl-*N*,*N*-dimethylaniline, E_{ox} ≈ 1.1 V *vs.* SCE in acetonitrile)[19] should provide an approximate value. The Coulomb term C was taken as –0.06 eV. With these data the driving force for PET was estimated as ΔG ≈ +0.55 eV for **FL-DTEo** and ΔG ≈ +0.05 eV for **FL-DTEc**. Hence, PET seems unlikely to play a role. Noteworthy, the **FL-DTEo** dyad shows no diminishing of the fluorescence quantum yield as compared to **FLm**, corroborating the absence of quenching (i.e., PET).

References

1. Kucherak, O. A.; Didier, P.; Mèly, Y.; Klymchenko, A. S. Fluorene Analogues of Prodan with Superior Fluorescence Brightness and Solvatochromism. *J. Phys. Chem. Lett*. **2010**, *1*, 616–620.
2. Baraldi, P. G.; Tabrizi, M. A.; Preti, D.; Bovero, A.; Romagnoli, R.; Fruttarolo, F.; Zaid, N. A.; Moorman, A. R.; Varani, K.; Gessi, S.; Merighi, S.; Borea, P. A. Design, Synthesis, and Biological Evaluation of New 8-Heterocyclic Xanthine Derivatives as Highly Potent and Selective Human A_{2B} Adenosine Receptor Antagonists. *J. Med. Chem*. **2004**, *47*, 1434–1447.
3. Kim, H. M.; Jung, C.; Kim, B. R.; Jung, S.-Y.; Hong, J. H.; Ko, Y.-G.; Lee, K. J.; Cho, B. R. Environment-Sensitive Two-Photon Probe for Intracellular Free Magnesium Ions in Live Tissue. *Angew. Chem. Int. Ed*. **2007**, *46*, 3460–3463.
4. Lei, S.; Heyen, A. Ver; De Feyter, S.; Surin, M.; Lazzaroni, R.; Rosenfeldt, S.; Ballauff, M.; Lindner, P.; Mössinger, D.; Höger, S. Two-Dimensional Oligo(phenylene-

ethynylene-butadiynylene)s: All-Covalent Nanoscale Spoked Wheels. *Chem. Eur. J.* **2009**, *15*, 2518–2535.

5. (a) Liddell, P. A.; Kodis, G.; Moore, A. L.; Moore, T. A.; Gust, D. Photonic Switching of Photoinduced Electron Transfer in a Dithienylethene-Porphyrin-Fullerene Triad Molecule. *J. Am. Chem. Soc*. **2002**, *124*, 7668–7669. (b) Bälter, M.; Li, S. M.; Nilsson, J. R.; Andréasson, J.; Pischel, U. An All-Photonic Molecule-Based Parity Generator/Checker for Error Detection in Data Transmission. *J. Am. Chem. Soc*. **2013**, *135*, 10230-10233.
6. Xie, H.; Ng, D.; Savinov, S. N.; Dey, B.; Kwong, P. D.; Wyatt, R.; Smith, A. B.; Hendrickson, W. A. Structure-Activity Relationships in the Binding of Chemically Derivatized CD4 to gp120 from Human Immunodeficiency Virus. *J. Med. Chem*. **2007**, *50*, 4898–4908.
7. Brouwer, A. M. Standards for photoluminescence quantum yield measurements in solution (IUPAC Technical Report). *Pure Appl. Chem.* **2011**, *83*, 2213–2228.
8. Frisch, M. J.; Trucks, G. W.; Schlegel, H. B.; Scuseria, G. E.; Robb, M. A.; Cheeseman, J. R.; Scalmani, G.; Barone, V.; Petersson, G. A.; Nakatsuji, H.; et al. *Gaussian 16, Revision A.03*, Gaussian, Inc., Wallingford CT, 2016.
9. Yanai, T.; Tew, D. P.; Handy, N. C. A new hybrid exchange–correlation functional using the Coulomb-attenuating method (CAM-B3LYP). *Chem. Phys. Lett.* **2004**, *393*, 51–57.
10. Tomasi, J.; Mennucci, B.; Cammi, R. Quantum Mechanical Continuum Solvation Models. *Chem. Rev.* **2005**, *105*, 2999–3093.
11. Preus, S. *a|e-UV-Vis-IR Spectral Software 1.2*, FluorTools, www.fluortools.com (accessed July 2, 2020).
12. Valeur, B.; Berberan-Santos, M. N. Chapter 8: Excitation Energy Transfer. In *Molecular Fluorescence,* 2nd Edition; Wiley-VCH: Singapore 2013; pp 213–262. ISBN: 978-3-527-32837-6
13. Casida, M. E. *Recent Advances in Density Functional Methods, Vol. 1*. Delano P. Chong Ed; World Scientific Publishing Co. Pte. Ltd. Singapore 1995. ISBN: 978-981-02-2442-4.
14. Martin, R. L. Natural transition orbitals. *J. Chem. Phys.* **2003**, *118*, 4775–4777.
15. (a) Heller, H. G.; Langan, J. R. Photochromic Heterocyclic Fulgides. Part 3. The Use of *(E)-α-(2.5*-Dimethyl-3-furylethylidene)(isopropylidene)succinic Anhydride as a

Simple Convenient Chemical Actinometer. *J. Chem. Soc., Perkin Trans. 2* **1981**, 341–343; (b) Yokoyama, Y., Hayata, H.; Ito, H.; Kurita, Y. Photochromism of a Furylfulgide, 2-[1-(2,5-Dimethyl-3-furyl)ethylidene]-3-isopropylidenesuccinic Anhydride in Solvents and Polymer Films. *Bull. Chem. Soc. Jpn.* **1990**, *63*, 1607–1610; (c) Glaze, A. P.; Heller, H. G.; Whittall, J. Photochromic Heterocyclic Fulgides. Part *7*. (*E*)-Adamantylidene-[1-(2,5-dimethyl-3-furyl)ethylidene]succinic Anhydride and Derivatives: Mode1 Photochromic Compounds for Optical Recording Media. *J. Chem. Soc., Perkin Trans. 2* **1992**, 591–594 and (d) Boule, P.; Pilichowski, J. F. Comments about the use of Aberchrome^{TM} 540 in chemical actinometry. *J. Photochem. Photobiol. A: Chem* **1993**, *71*, 51–53.

16. (a) Terenziani, F.; Katan, C.; Badaeva, E.; Tretiak, S.; Blanchard-Desce, M. Enhanced Two-Photon Absorption of Organic Chromophores: Theoretical and Experimental Assessments. *Adv. Mat.* **2008**, *20*, 4641–4678 and (b) Rumi, M.; Perry, J. W. Two-photon absorption: an overview of measurements and principles. *Adv. Opt. Photon.* **2010**, *2*, 451–518.
17. Kleinwächter, M.; Teichmann, E.; Grubert, L.; Herder, M.; Hecht, S. Oxidative and reductive cyclization in stiff dithienylethenes. *Beilstein J. Org. Chem.* **2018**, *14*, 2812–2821.
18. Greenfield, S. R.; Svec, W. A.; Gosztola, D.; Wasielewski, M. R. Multistep Photochemical Charge Separation in Rod-like Molecules Based on Aromatic Imides and Diimides. *J. Am. Chem. Soc.* **1996**, *118*, 6767–6777.
19. Luo, P.; Feinberg, A. M.; Guirado, G.; Farid, S.; Dinnocenzo, J. P. Accurate Oxidation Potentials of 40 Benzene and Biphenyl Derivatives with Heteroatom Substituents. *J. Org. Chem.* **2014**, *79*, 9297–9304.